0254-6124/2011/31(2)-125–25 *Chin. J. Space Sci.* 空间科学学报

R. A. Wolf. Theories and simulations in substorm research: A review. *Chin. J. Space Sci.*, 2011, **31**(2): 125-149

Theories and Simulations in Substorm Research: A Review *

R. A. WOLF

(*Physics and Astronomy Department, Rice University, Houston, Texas,* 77251-1892*, USA*)

Abstract Both theory and simulation have played important roles in defining and illuminating the key mechanisms involved in substorms. Basic theories of magnetic reconnection and of interchange and ballooning instabilities were developed more than 50 years ago, and these plasma physical concepts have been central in discussions of substorm physics. A vast amount of research on reconnection, including both theoretical and computational studies, has helped provide a picture of how reconnection operates in the collisionless environment of the magnetosphere. Still, however, we do not fully understand how key microscale processes and large-scale dynamics work together to determine the location and rate of reconnection. While in the last twenty years, it has become clear that interchange processes are important for transporting plasma through the plasma sheet in the form of bursty bulk flows and substorm expansions, we still have not reached the point where simulations are able to realistically and defensibly represent all of the important aspects of the phenomenon. More than two decades ago it was suggested that the ballooning instability, the basic theory for which dates from the 1950s, may play an important role in substorms. Now the majority of experts agree that regions of the plasma sheet are often linearly unstable to ideal-MHD ballooning. However, it is also clear that kinetic effects introduce important modifications to the MHD stability criterion. It is still uncertain whether ballooning plays a leading role in substorms or has just a minor part. Among the different types of simulations that have been applied to the substorm problem, global MHD codes are unique in that, in a sense, they represent the entire global substorm phenomenon, including coupling to the solar wind and ionosphere, and the important mechanisms of reconnection, interchange, and ballooning. However, they have not yet progressed to the point where they can accurately represent the whole phenomenon, because grid-resolution problems limit the accuracy with which they can solve the equations of ideal MHD and the coupling to the ionosphere, and they cannot accurately represent small-scale processes that violate ideal MHD.

Key words Substorm, Reconnection, Interchange, Simulations

Classified Index P353

1 Introduction

For the purposes of this paper, we define "theory" to be the use of mathematics to solve equations representing well-founded laws of physics, in order to describe an idealized physical system designed to capture the essence of an observed physical phenomenon while maintaining mathematical tractability. Ideally, the theory itself is rigorous and logical. The main problem is that the simplifying assumptions and idealizations needed to make the problem tractable often produce results that depart from real-world observa-

∗ This work was supported by the NASA Heliospheric Theory Program under grant NNX08AI55G

Received January 16, 2011

E-mail: rawolf@rice.edu

tions. My operational definition of "simulation" is almost the same as that of "theory", except that the mathematical treatment centers on the use of computers to solve numerical approximations to the basic physical equations (usually differential equations). Ideally, the computational physicist responsible for the simulation makes sure that the essential results are insensitive to the details of the numerical method used, although I suspect there have been instances where published analytic theories and computer simulations have fallen somewhat short of the above-described standards of rigor and numerical accuracy.

While theory and simulation have played important roles in substorm research, it must be admitted that data analysis has always been the main driver of the field. The primary disputes have always been about how to interpret observations. As a result, the principal combatants in the big and central arguments concerning the nature of substorms have generally been data analysts, not theorists or computational physicists. Substorm research has never been about highly speculative mathematical theories confronting solid, indisputable scientific observations. It has sometimes involved solidly logical (though simplified and idealized) theories confronting questionable observational results.

Figure 1 illustrates an allegory of our situation. Observers are desperately paddling around in an Ocean of Data, trying to reach the mainland (*i.e.*, trying to figure out how substorms actually work). Different groups of theorists stand on different islands of solid theory. (There is a ballooning island, a reconnection island, *etc.*) Theorists work to enlarge their islands while staying out of trouble with the observers. Most substorm researchers, both theorists and observers, are pretty sure that they can see the mainland, but everybody thinks it is in a different direction. Currently, nobody is strong enough to swim directly to the mainland. However, an observer can choose an island that he or she believes is solid and walk across it, hoping to get closer to the mainland. That is, the theoretical islands give the observers ide-

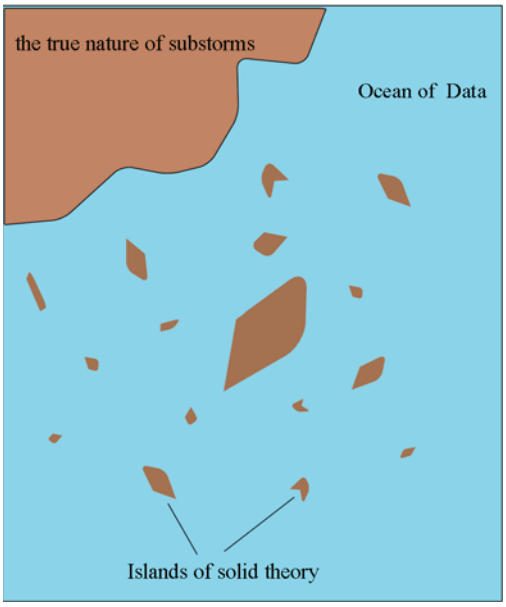

Fig. 1 The role of theory in substorm research

as that help them frame interpretations of their data. The long-term hope is that the relevant islands will get big enough and cohere so that most of us can get to the mainland. It's highly likely that some of the theoretical islands will turn out to be irrelevant, but we don't know which ones.

The rest of this paper describes what different sets of theorists have done to enlarge their islands. For practical purposes, I have chosen to concentrate on just four islands on which there has been a substantial amount of theoretical effort, involving three physical processes suggested to have major roles in substorms and a numerical approach that provides an overall picture of the phenomenon.

2 Magnetic Reconnection

2.1 Reconnection Theory Before 1973

I first discuss the development of the theory of reconnection before the explosion of interest in the subject associated with the introduction of the near-Earth-neutral-line model of substorms. Figure 2 illustrates the concept of reconnection. The top diagram shows two magnetic field lines (AB and CD) interacting and forming a new pair of field lines AC and BD.

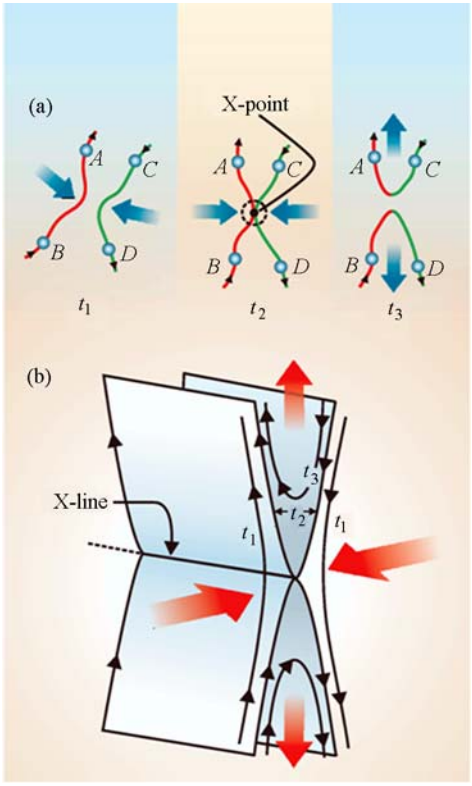

Fig. 2 Concept of reconnection (From Schwarzschild[1], adapted from Paschmann[2])

A 2D version of reconnection is shown in Figure 2(b).

The idea of reconnection in a space physics context began with Giovanelli[3] and Hoyle[4], who suggested the conversion of magnetic energy to particle energy at a magnetic null point as a mechanism for solar flares. Dungey[5] used MHD to show that a plasma could collapse to a thin current sheet near a magnetic neutral point. He pointed out that magnetic field lines could be broken and rejoined, and he suggested reconnection as a possible explanation for the aurora. However, his proof was highly idealized, because it assumed negligible plasma pressure. Furth *et al.*[6] developed a full quantitative theory of resistive tearing, confirming Dungey's conclusion that a tearing-type perturbation in a neutral sheet would grow in time. Figure 3 shows the situation, which was studied using a linear analysis of a perturbation that was periodic in the x-dimension and exponentially growing in time, imposed on a configuration with a

Fig. 3 Development of a tearing mode in a neutral sheet. Solid arrows are flow velocities. Here and elsewhere in this paper, x is toward the Earth, z is northward, and y is toward dusk (Adapted from Furth *et al.*[6])

central neutral sheet.

One reason why reconnection in space plasmas has been a profoundly difficult theoretical problem is that both large- and small-scale processes play absolutely essential roles. From the perfect-conductivity relation

$$\boldsymbol{E} + \boldsymbol{v} \times \boldsymbol{B} = 0, \tag{1}$$

and Faraday's law, one can prove that if two fluid elements initially share a field line, they will forever share the same field line (*e.g.*, Siscoe[7]). The situations shown in Figure 2 and Figure 3 obviously violate that condition, so apparently they can only occur if there are violations of the perfect-conductivity relation, which is a central assumption of ideal MHD. Therefore, reconnection cannot occur in ideal MHD, which is the simplest representation of large-scale plasma behavior. Furthermore, the simplest kind of violation of ideal MHD, the addition of a Coulomb-collisional resistivity term to the ideal Ohm's law, does not result in appreciable reconnection in the magnetosphere, because collisions in charged particles are so rare as to be irrelevant. If reconnection is to occur in the magnetosphere, it requires the operation of small-scale plasma processes. On the other hand, it was realized very early that boundary conditions could make a big difference. Sweet[8] and Parker[9] suggested a mechanism in which the frozen-in-flux condition was violated across a magnetic-field-free neutral sheet that extended for a distance that was comparable to the dimension of the macroscopic system, but the resulting reconnection rate turned out to be too slow to be important for solar-system

applications. Petschek[10] proposed a reconnection theory in which the dimensions of the region of frozen-in-flux violation were much smaller than dimensions of the overall system, and magnetic tension created exhaust plumes (left and right in Figure 4); the reconnection rate for this geometry proved to be much faster. This finding demonstrated that large-scale dynamics, which determines the boundary conditions, plays a crucial role in determining the rate of the process.

Although much of the theory of reconnection before 1973 was developed for application to the Sun and for controlled-fusion devices, the concept of reconnection was also applied to the magnetosphere. In a famous paper, Dungey[12] suggested that reconnection drives magnetospheric convection, and Coppi *et al.*[13] suggested that the tearing mode would operate in the center of the current sheet in the Earth's magnetotail. These two landmark papers provided a theoretical framework for the development of the near-Earth-neutral-line model of substorms (Russell and McPherron[14]; McPherron *et al.*[15]), which was a phenomenological picture based on the interpretation of observations.

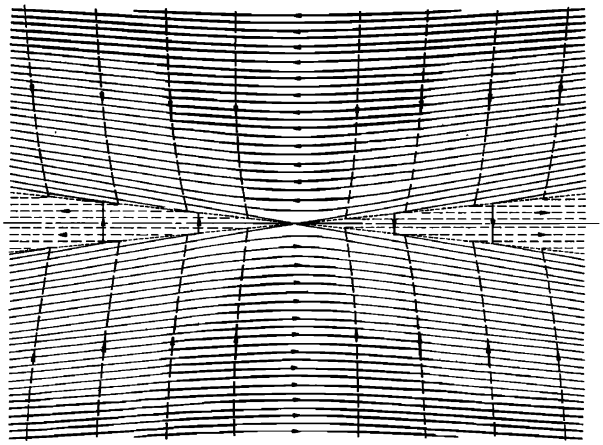

Fig. 4 Petschek model of reconnection. Solid lines with arrows are magnetic field lines, while dashed lines with arrows are flow lines. Ideal MHD holds except in a small "diffusion region" at the center of the diagram (From Vasyliunas[11])

2.2 Post-1973 Reconnection Theory With no Background B_y or B_z

By the time of Vasyliunas' review[11] of the theory of reconnection, it had become clear that major violation of the ideal Ohm's law in a collisionless plasma was limited to a small "diffusion box", where electrons are demagnetized and can be accelerated in the direction opposite to the electric field; in this region, electron inertial effects become important. Only a small amount of fluid traverses that box. It was also clear that the reconnection rate could vary from low values to values greater than the external Alfvén speed, depending on the boundary conditions.

For the simplest kind of collisionless reconnection, characterized by regions of oppositely directed magnetic field separated by a neutral sheet, many simulations have been carried out using different boundary conditions and different codes. Using the assumption of resistive MHD, *i.e.*,

$$\boldsymbol{E}+\boldsymbol{v}\times\boldsymbol{B}=\eta\boldsymbol{J}, \tag{2}$$

with resistivity η chosen to be much larger than the value estimated from simple Coulomb collisions, many simulations were carried out to determine the basic properties of reconnection in the near tail. In addition, fluid simulations were carried out with Hall MHD, which assumes

$$\boldsymbol{E}+\boldsymbol{v}\times\boldsymbol{B}=\eta\boldsymbol{J}+\frac{\boldsymbol{J}\times\boldsymbol{B}}{ne}, \tag{3}$$

and with fluid codes that include off-diagonal terms in the ion pressure tensor. Hybrid simulations (ions treated as particles, electrons as a fluid with and without electron mass and pressure anisotropy), and full electromagnetic particle simulations have also been used. The situation is terrifyingly complex, and it has been difficult for non-experts (including the present author) to develop a clear picture from this zoo of simulations, which were, to further complicate matters, typically carried out for different initial and boundary conditions.

However, about ten years ago a community exercise called the GEM Reconnection Challenge seemed to clarify things somewhat. Specialists in all of the major types of simulations agreed to perform simulations for the same set of initial and boundary conditions. They considered a uniform neutral sheet (specifically a Harris sheet (Birn *et al.*[16]) with anti-parallel field lines on the two sides of the current sheet). To this zero-order configuration, they added a small initial perturbation that created an X-line at the center of the simulation box. Periodic boundary conditions were assumed and each of the simulations used the same values for the ratio of the dimensions of the box relative to the initial thickness of the current sheet. The resistivity used in the MHD models was taken to be either uniform in space or, in some cases, spatially localized to regions where the current density exceeded a pre-determined threshold. Everybody plotted the reconnection rate as a function of time. Full-particle, hybrid, and Hall-MHD simulations all gave remarkably similar results, as shown in Figure 5. In resistive MHD simulations, the reconnection rate depended on the assumed resistivity. For uniform resistivity, the rate was always slower than that exhibited by the more detailed simulations, as shown in Figure 5. However, when MHD simulations were carried out assuming that the resistivity was zero unless the current density exceeded a preset threshold, the reconnection rates were substantially higher (Otto[17]).

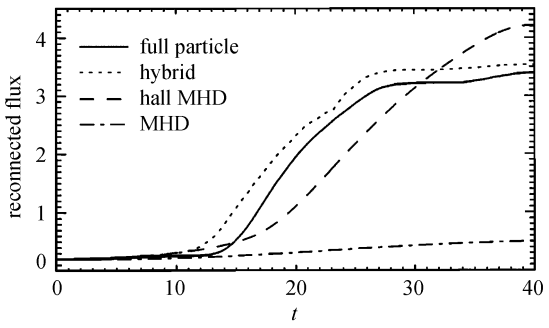

Fig. 5 Comparison of reconnection rates computed for the same conditions by four different methods, as indicated. The time unit is the ion gyrofrequency in the external field, and the flux unit is the product of the external magnetic field and the ion inertial length (From Birn *et al.*[16])

The physical picture that came out of the full-particle, hybrid, and Hall MHD simulations in the GEM Reconnection Challenge is illustrated in Figure 6. There is a tiny diffusion region near the neutral point (shown as the central red region of the diagram) where electrons are unlocked from the magnetic field, a situation that is represented by a resistivity in the fluid codes. In a larger surrounding region (shown in green), electrons are frozen to the field lines, but the ions are not, due to their larger mass. The result is standing whistler waves that involve non-zero currents in the plane of the picture (Shay *et al.*[18]; Birn *et al.*[16]) and magnetic fields perpendicular to that plane. These perturbation magnetic fields are a signature of the Hall effect and do not occur in ideal MHD.

The results of the GEM Reconnection Challenge

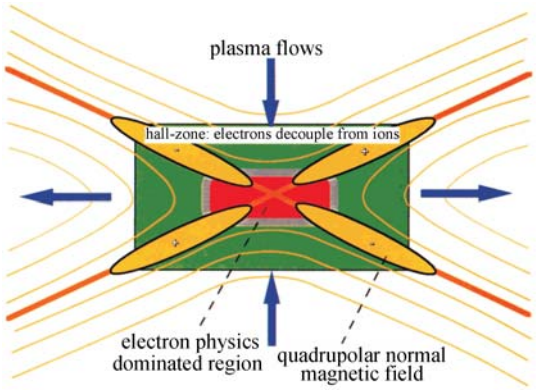

Fig. 6 Physical picture of reconnection that came from the GEM Reconnection Challenge. The plane of the picture is the plane that contains the magnetic field lines in the initial situation before reconnection starts. Electron physics dominates the red "diffusion region", while ions decouple from the electrons in the green "Hall zone". Within the Hall zone, currents flow in the plane of the picture within the yellow regions, causing magnetic field perturbations perpendicular to the page (From Hesse *et al.*[19])

appeared for a time to pretty much settle the matter of how reconnection occurs in a simple Harris sheet, at least for parameter values that are reasonable for the inner plasma sheet. That picture's basic prediction of Hall-current wings on the reconnection region has been confirmed observationally (see Asano *et al.*[20] and references therein). However, some evidence has recently appeared indicating that the GEM-Challenge picture may, in fact, be too simple (Hesse *et al.*[21]).

My discussion of reconnection so far has been confined to the simple case where the magnetic fields on the two sides of the neutral sheet are anti-parallel, at least in regions far from the X-line. However, reconnection frequently occurs in situations that are far from that anti-parallel situation. Gosling *et al.*[22] in fact showed that, in the solar wind, reconnection happens mainly at discontinuities where the magnetic field directions on the two sides of the current sheet differ by less than 90°. In the magnetotail, magnetic fields in the northern and southern tail lobes, projected onto the plane of the cross-tail current sheet, are not typically exactly anti-parallel, and the magnetic field in the center of the current sheet is not exactly zero, so it was clear many years ago that the theory of reconnection had to be generalized to include more general geometries than the situation considered in the present section. I divide the discussion into two parts: the case where the magnetic field in the center of the current sheet has a component in the direction of the current (called a "guide field") and the case where the initial magnetic field in the center of the current sheet has a component perpendicular to the cross-tail current (in the plane of Figure 6). I consider the guide field first.

2.3 Effect of a Guide Field (B_y)

When realistic geometries are considered, we immediately encounter questions about the definition of reconnection. For example, consider the situation depicted in Figure 7(a), which shows the magnetospheric xz plane. According to the definition of Vasyliunas[11], reconnection occurs if there is flow across the separatrix between closed field lines that connect to the Earth and plasmoid field lines, which close on themselves without encountering the Earth. Now suppose that we add a finite B_y component to the simple 2D situation such that now Figure 7(a) shows just the x- and z-components of the magnetic field. If the reconnection occurs over a finite distance in y, then the actual situation is as depicted in Figure 7(b). What looks like an unconnected plasmoid in 2D projection (Figure 7a) is actually magnetically connected to the Earth. What looks to be a plasmoid in a 2D projection is actually a flux rope when seen in 3D. A field line connects to the Earth with one footpoint in the southern ionosphere, spirals its way through the flux rope structure that appears like a plasmoid in 2D, and has another footpoint in the

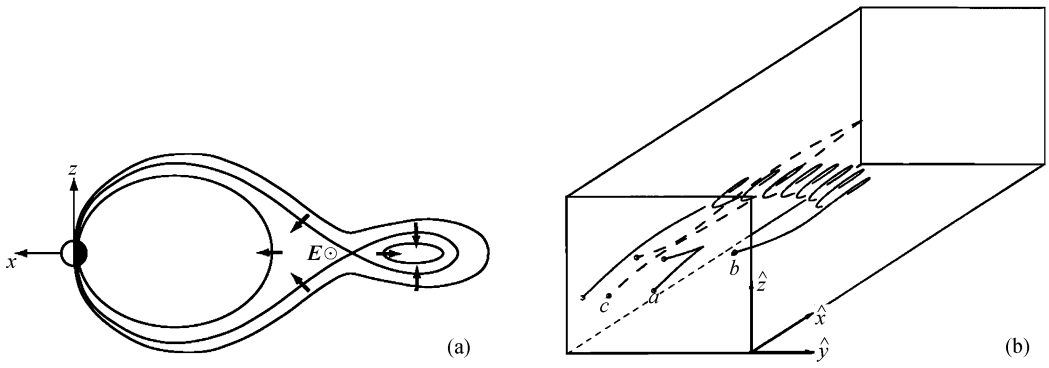

Fig. 7 (a) Magnetic field lines on the xz-plane. (b) 3D view of magnetic field lines, in a case where there is a finite positive B_y in the current sheet, and reconnection occurs along a finite length in the y-direction. Heavy arrows in the left diagram are flow directions. Right diagram is from Schindler *et al.*[23]

northern ionosphere. In this case, all of the field lines are closed, and it is not apparent that they can be described as having different topologies. Although we would like to be able to refer to a situation like that shown in Figure 7 as "reconnection", it is not obvious how we can do so following Vasyliunas' definition without introducing a creative definition of "topology".

Axford[24] suggested a more general definition of reconnection as a localized violation of the ideal Ohm's law, and Hesse and Schindler[25] worked out a detailed description of the properties of reconnection following this definition. This definition includes the cases covered by *Vasyliunas*' definition, which involve an electric field at a magnetic neutral point, as well as the case shown in Figure 7, where $\boldsymbol{E}\cdot\boldsymbol{B}\neq 0$. However, it also includes the case where the magnetic field is uniform but there is an electric field parallel to it (as is the case in the auroral acceleration region above Earth's ionosphere). That situation "feels different" than the X-line reconnection shown in Figure 7, and it ought to be possible to distinguish these cases by different names. However, to date, there does not seem to be any generally accepted convention on how to do this.

One might at first think that the addition of a guide field would dramatically reduce reconnection: the argument presented in Section 2.2 suggests that reconnection depends on the existence of a region where even electrons are demagnetized, and the presence of non-zero B_y at the center of the current sheet eliminates that possibility. However, detailed theoretical work indicates that the guide field has only a rather mild effect on reconnection and can actually make it proceed faster (*e.g.*, Hesse *et al.*[26]; Pritchett and Coroniti[27]). The crucial region near the neutral line, where an electric field can accelerate electrons freely along the neutral line, is now replaced by a region with $\boldsymbol{B}$ directed along the y-axis, where an electric field parallel to $\boldsymbol{B}$ can accelerate the electron freely.

2.4 Effect of a Positive B_z in the Initial Configuration

The question here is: How can reconnection occur in a configuration like that shown in Figure 8, which resembles the real plasma sheet? Again, the answer depends on the definition of "reconnection". Using Axford's definition, reconnection occurs if there is any violation of the ideal Ohm's law, which means that even simple gradient and curvature drift give rise to reconnection. This definition, under which reconnection is always present in the plasma sheet, is not useful for substorm discussions. In substorm physics, the term "reconnection" is reserved for a configuration like that shown in Figure 7(a), which involves magnetic fields of different signs perpendicular to the current sheet on either side of a neutral line. In other words, it is convenient to adopt the Vasyliunas definition, defining the topology of a field line in terms of the number of times it crosses the center of the current sheet.

Taking that definition of reconnection, which is what I do in the rest of this paper, it is clear that an infinitesimal perturbation in the magnetic field of Figure 8 does not immediately imply reconnection. The question then arises: Is there a physical process that can cause a configuration like that shown in Figure 8 to develop a region of near-zero B_z across the neutral sheet and then another process that causes reconnection to proceed, or are both parts of the evolution dominated by the same process?

Within the context of resistive MHD the answer is clearly the second. Beginning in the late 1980's, Joachim Birn and Michael Hesse used resistive MHD simulations and sometimes quasi-static equilibrium

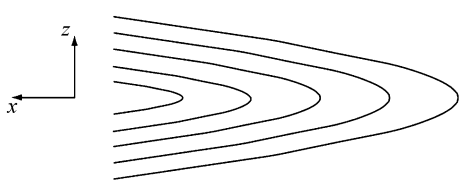

Fig. 8 Current sheet with positive B_z across it

solutions to produce stretched tail-like configurations that were designed to represent the inner and middle magnetosphere under growth-phase conditions. They used a rectangular simulation box designed to exclude the inner magnetosphere and magnetopause boundary layers. Some conclusions are the following.

(1) Reconnection can occur if B_z is sufficiently small, the current sheet is sufficiently thin, and an appropriate amount of resistivity is assumed.

(2) The observation-based picture (McPherron *et al.*[15]) that reconnection leads to the formation of a substorm current wedge was confirmed by the MHD simulations (Hesse and Birn[28]).

(3) The current in the substorm wedge is mainly driven by pressure gradients (Birn and Hesse[29]).

(4) Current sheet thinning can be caused by a variety of circumstances (Birn *et al.*[30]).

(5) A perturbation at the magnetopause boundary can lead to a very thin current sheet and loss of equilibrium (Birn *et al.*[31]).

(6) Reconnection has only a small effect on the total entropy of a flux tube, because the diffusion box, where dissipation occurs and entropy presumably rises, is so small that only a small fraction of the fluid elements in a flux tube traverse it (Birn *et al.*[32]).

Using kinetic theory to try to understand the nature of the process that violates ideal MHD to cause reconnection in the plasma sheet raises profound questions, with analytic theory and PIC simulations not always in total agreement. Schindler[33] argued that an ion tearing mode should occur when ions become demagnetized, i.e., when their gyroradii become comparable to or greater than the radius of curvature of field lines crossing the current sheet. Galeev and Zelenyi[34] showed that the magnetized electrons could stabilize the ion tearing mode. Lembege and Pellat[35], Pellat *et al.*[36], Brittnacher *et al.*[37], Quest *et al.*[38], and Schindler[39] showed that the ion tearing mode should be universally stable when there is initially a substantial normal component of $\boldsymbol{B}_z$. Sitnov and Schindler[40] have recently argued for the destabilization of the tearing mode near the tailward end of a thin current sheet. Despite the fact that the efficacy of ion tearing in the presence of finite normal component of $\boldsymbol{B}$ is still unclear from the viewpoint of analytic theory, it seems to occur regularly in PIC simulations (*e.g.*, Pritchett *et al.*[41], Pritchett[42]), which should fully include kinetic effects, though with an unrealistic ratio of ion to electron mass.

2.5 Summary Comment

Despite many years of intense effort and considerable progress toward understanding, it is still not clear how reconnection happens in the collisionless plasma sheet, and how small-scale and large-scale processes work together to determine the rate of reconnection.

3 Interchange, Entropy, Bubbles, Pressure Crisis, and Substorms

3.1 Interchange Instability, $PV^{5/3}$, and Entropy

The basic theory of the interchange instability goes back to the early days of plasma physics (Rosenbluth and Longmire[43]). It was applied early to Earth's inner magnetosphere by Sonnerup and Laird[44] and others, but the plasma sheet is where interchange processes seem to be most important. The energy principle of ideal MHD implies that a plasma system that is at rest and in force equilibrium is unstable if an exchange of two unit flux tubes (and the plasma frozen to them) produces a decrease of the potential energy of the system. (The situation is illustrated schematically in Figure 9) If the exchange is carried out so that the volume initially occupied by flux tube 1 equals the volume occupied by flux tube 2 in the final state, and vice versa, then the criterion for instability can be expressed as

$$\frac{\delta V}{V}\frac{\delta(PV^{5/3})}{PV^{5/3}} < 0 \tag{4}$$

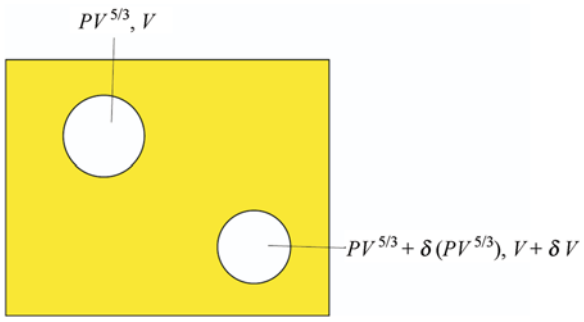

Fig. 9 Diagram of simple interchange viewed in a plane perpendicular to the local magnetic field. The two white tubes are interchanged, without disturbing the yellow background

(Schmidt[45]), where $V = \int \mathrm{d}s/B$ is the volume of a flux tube containing one unit of magnetic flux. If the exchange is between two adjacent flux tubes, and they are allowed to expand and contract in equal amounts to minimize the final energy, the criterion takes the more general form originally derived by Bernstein *et al.*[46]:

$$\left(\frac{\delta V}{V} - \frac{\mu_o \delta P}{V}\int \frac{\mathrm{d}s}{B^3}\right)\frac{\delta(PV^{5/3})}{PV^{5/3}} < 0. \qquad (5)$$

The δP term is important only in high-β plasmas. However, even in the high-β plasma sheet, gradients in V and P are usually approximately antiparallel, so (5) normally reduces to (4). Xing and Wolf[47] showed that (4) can be generalized to a form $\nabla V \cdot \nabla(PV^{5/3}) < 0$, for low-$\beta$ conditions. Thus, a system is unstable to interchange if $PV^{5/3}$ decreases along the direction of increasing flux tube volume V.

Following Birn *et al.*[32], we note that the parameter $P^{3/5}/\rho$ is directly proportional to $e^{\sigma/R}$, where σ is the entropy per unit mass of an ideal gas and R is a constant. The flux tube integral

$$\Sigma = \int \left(\frac{P^{3/5}}{\rho}\right)\rho \mathrm{d}s/B \qquad (6)$$

is conserved as a flux tube drifts, provided that the entropy per unit mass is conserved and the mass elements $\rho \mathrm{d}s/B$ are frozen to the magnetic field. If the system is also at equilibrium, so that pressure is constant along a magnetic field line, then the parameter $PV^{5/3}$, which plays the central role in the criterion for interchange instability, is conserved. In my discussion, I use $PV^{5/3}$ as shorthand for the more general conserved quantity $\Sigma^{5/3}$.

3.2 Pressure Balance Inconsistency

Observations show that there is a systematic sunward flow of plasma through the auroral ionosphere, which implies a dawn-to-dusk electric field in the equatorial region of the magnetosphere. Most theorists originally pictured the transport of plasma in the plasma sheet in terms of uniform earthward flow, although with significant perturbations. If $PV^{5/3}$ is approximately conserved along a drift path and flow in the plasma sheet is consistently earthward, we would expect $PV^{5/3}$ to be approximately uniform within the plasma sheet. However, observation-based statistical models of the plasma and magnetic field indicate that this is not the case (Erickson and Wolf[48]), with $PV^{5/3}$ systematically decreasing as one moves Earthward. That realization gave rise to a quandary called the "pressure balance inconsistency" or "pressure crisis", though "entropy inconsistency" or "entropy crisis" would have been better names. Figure 10 illustrates the problem: the

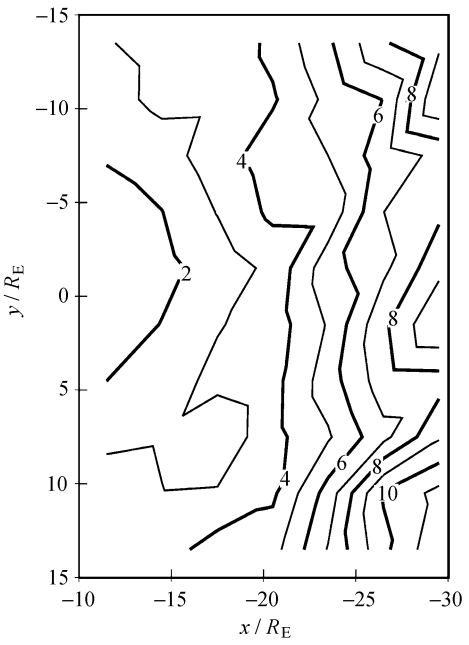

Fig. 10 Average value of ion $PV^{5/3}$ in units of 10^{16} Pa·m^3/Wb, in the equatorial plane, computed from Geotail data (From Kaufmann *et al.*[49])

observed $PV^{5/3}$, based on statistical models, consistently decreases earthward and by a substantial factor.

One obvious mechanism for the earthward decrease of $PV^{5/3}$ in the plasma sheet is loss of plasma from the flux tube by precipitation into the ionosphere. However, since the strong-pitch-angle-scattering lifetime for loss by ions in the middle plasma sheet is much longer than the average convection time through the medium, it would be difficult for a large fraction of ions to be lost from flux tubes in the region shown in Figure 10. A significant fraction of the electrons could be lost, but that would not decrease the total pressure much, since electrons contribute only about 1/8 of the total pressure (Baumjohann *et al.*[50]). A second simple loss mechanism is gradient and curvature drift out the sides of the tail (Tsyganenko[51]; Spence and Kivelson[52]; Wang *et al.*[53]). It is always non-negligible and may solve the problem in times of slow convection. However, it is difficult to imagine how it could eliminate the inconsistency in times of strong convection: in steady convection, an ion gradient/curvature drifting across the width of the tail gains energy equal to its charge times the cross-tail potential drop; the average ion energy in the dusk-side plasma sheet is much less than the potential drop; thus it is hard to see how the majority of the plasma sheet ions could have drifted all of the way across the tail and out through the magnetopause. As discussed in the next section, resolution of the pressure balance inconsistency seems to require a more subtle mechanism, at least during times of strong convection.

3.3 Bubbles and Blobs

In Earth's plasma sheet, interchange instability is usually observed in its nonlinear development, and not in its linear phase. It is useful to characterize the nonlinear development in terms of bubbles (flux tubes that have lower $PV^{5/3}$ than their surroundings) and blobs (flux tubes that have higher $PV^{5/3}$ than their surroundings). Consider a bubble that is initially at rest in the plasma sheet as shown schematically in Figure 11. Because it has lower $PV^{5/3}$ than its neighbors, the bubble carries less gradient/curvature drift current than its surroundings, causing positive charges to build up on the dawn side of the bubble and negative charges on the dusk side. The enhanced dawn-to-dusk electric field inside the bubble causes it to start to $\boldsymbol{E} \times \boldsymbol{B}$ drift earthward, launching Alfvén waves toward the northern and southern ionospheres, which eventually produce Birkeland currents down to the ionosphere on the dawn side, and up on the dusk side. After the system settles down in a few Alfvén-wave travel times, the interruption in the cross-tail current caused by the bubble will be completed by dawn-to-dusk current across the local ionosphere. Using similar physical arguments it can be seen that a blob will move tailward, toward the region of higher flux tube volume.

Pontius and Wolf[54] suggested the existence of earthward-moving bubbles in the plasma sheet at about the same time that observations revealed the existence of mostly-earthward-moving bursty bulk flows (BBF's) in the plasma sheet (Baumjohann *et al.*[55]; Angelopoulos *et al.*[56]; Angelopoulos[57]). The association between bubbles and BBFs was established (Chen and Wolf[58]; Sergeev *et al.*[59], Kauristie *et al.*[60], Nakamura *et al.*[61]), and it became clear that a large fraction of the total transport in the plasma sheet occurred in BBF's (Angelopoulos *et al.*[56]).

Chen and Wolf[62] calculated the motion of a highly idealized version of a bubble, namely a

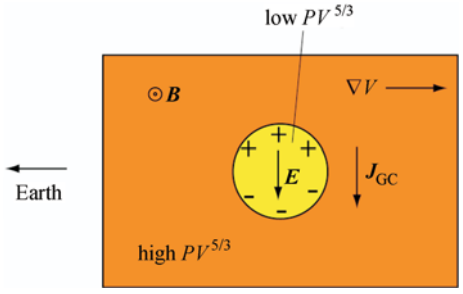

Fig. 11 Cartoon in the xy plane showing why a bubble tends to move earthward in Earth's plasma sheet

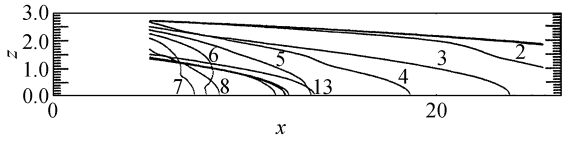

Fig. 12 Evolution of a filament that originally extended to 40 R_E with $PV^{5/3}$ equal to 34% of the local background. The small numbers are times in minutes. The heavy line indicates the final equilibrium shape (From Chen and Wolf[62])

thin, ideal-MHD filament that slips without friction through a background medium. Figure 12 shows the evolution of a filament that started at rest with a tailward extent of 40 R_E and the same shape as its neighbors, but with $PV^{5/3}$ equal to 34% of the local background. The bubble accelerated earthward until it encountered background flux tubes with $PV^{5/3}$ predominantly lower than its value, when it began to accelerate tailward. After a few oscillations, the bubble came to rest at an equilibrium position, where its $PV^{5/3}$ matched the neighboring tubes. Such oscillations have now been observed (Panov *et al.*[63]). Meanwhile, Birn *et al.*[64–65] carried out full 3D bubble simulations, which indicate similar behavior but also display spatial structure that the thin-filament calculations cannot describe (see Figures 13 and 14).

More detailed simulations are shedding additional light on these processes. Pritchett and Coroniti[66] found that interchange fingers developed in a full electromagnetic particle simulation. 3D particle simulations by Sitnov *et al.*[67] implied that the leading edge of a dipolarization forms a sharp "dipolarization front", and that phenomenon has been observed by Runov *et al.*[68] with the predicted characteristics.

Three mechanisms have been suggested for creating bubbles.

(1) Due to non-uniformities in the tail lobe, new closed plasma-sheet field lines created at a far-tail X-line may be created with different values of $PV^{5/3}$. These non-uniformities seem likely to result from the patchy nature of reconnection at the dayside magne-

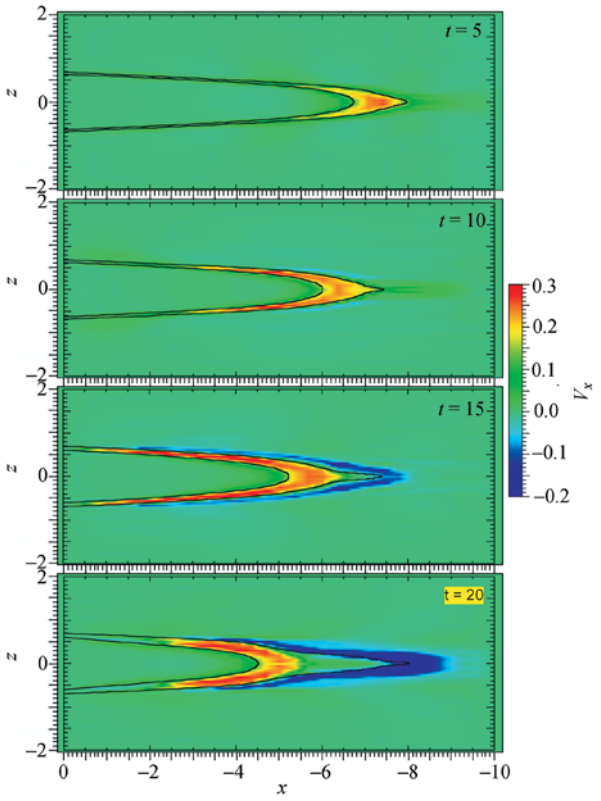

Fig. 13 Velocity in and around a bubble as a function of time, as derived from a 3D MHD simulation. The black curves represent the boundaries of the bubble in the xz plane, as it evolved in time. Units of time, distance, and velocity are arbitrary (From Birn *et al.*[64])

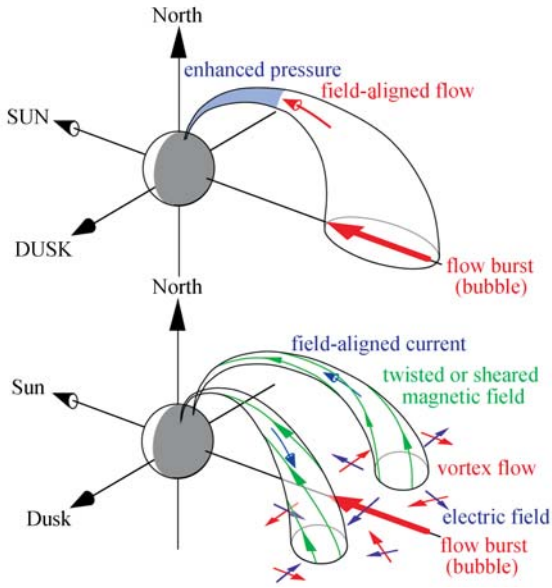

Fig. 14 Cartoon of an earthward-moving bubble based on 3D MHD simulations (From Birn *et al.*[64])

topause, as exemplified by flux transfer events.

(2) A localized reconnection region within the plasma sheet divides the entropy on a closed flux tube into two parts, a new and shorter closed flux tube and a plasmoid. Since some of the entropy goes to the plasmoid, the shortened closed flux tube has lower $PV^{5/3}$ than the original one.

(3) Suppose that thinning of the inner plasma sheet leads to a current density that is high enough to exceed some threshold (mechanism unspecified at this point), which leads to a violation of frozen-in flux and a localized electric field in the $+y$ direction (out of page in Figure 15), in the rest frame of the plasma. Field line 2 slips on the plasma and its equatorial crossing point moves earthward. The volume of flux tubes between lines 1 and 2 decreases, creating a bubble, and the volume between 2 and 3 increases, creating a blob. This mechanism, which bears some resemblance to the tail-current-disruption model of Lui[69], was studied quantitatively in 2D by Lee *et al.*[70−71], and recently in 3D by Yang *et al.*[72].

Production of bubbles in the plasma sheet by any or all of these three mechanisms helps to resolve the pressure balance inconsistency, because the interchange effect will cause bubbles to move preferentially

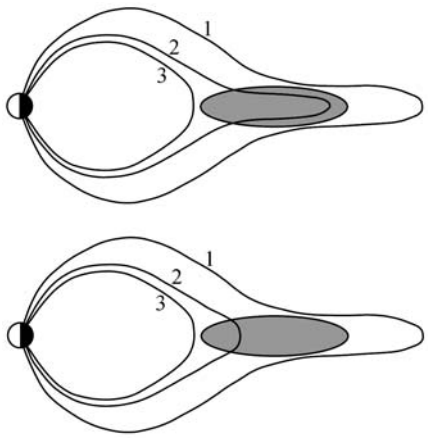

Fig. 15 Diagram showing how slippage of a field line (#2) on the plasma in a region of high current density (shaded region) can produce a bubble (between lines 2 and 3) and a blob (between lines 1 and 2). From Wolf *et al.*[73]

to the inner plasma sheet and blobs to the distant plasma sheet, resulting in a tailward gradient in the average $PV^{5/3}$. Once a bubble is created by any of these mechanisms, its motion can be represented by MHD, at least to first approximation. However, the mechanisms for creation of the bubbles all involve reconnection or other violations of ideal MHD, which means that some small-scale process must play a crucial role.

Notice that the idea of bubbles is in no way a competitor to the concepts of reconnection or current disruption. Bubbles result from both processes. The bubble concept provides a way of visualizing the motion, through the background medium, of a flux tube that has undergone current disruption or reconnection.

3.4 Relationship to Substorms

Assuming uniform, steady, strong, adiabatic, sunward convection on closed magnetic field lines from the distant tail to the inner plasma sheet in a model that maintains the magnetic field in force balance with the computed particle populations leads to a minimum in magnetic field strength in the inner plasma sheet, as illustrated in Figure 16. This conclusion has been verified by many calculations, both 2D (*e.g.*, Erickson[74]; Hau[75]) and 3D (*e.g.*, Toffoletto *et al.*[76]; Lemon *et al.*[77]). The reason is simple. Flux tube volume $V = \int \mathrm{d}s/B$ naturally increases rapidly with tailward distance, because the field lines get longer and the field normally gets weaker. On the other hand, the pressure in the tail lobes decreases relatively slowly with distance. Therefore, in statistical models, $PV^{5/3}$ normally increases with distance, as illustrated in Figure 10. In order to conserve $PV^{5/3}$, computational models with enforced earthward convection tend to create a region of very weak magnetic field near the center of the current sheet in the near-Earth region, in order to increase flux tube volume there. The computed inner-plasma-sheet magnetic field consequently gets very stretched, resembling the growth phase of a substorm. In model calculations

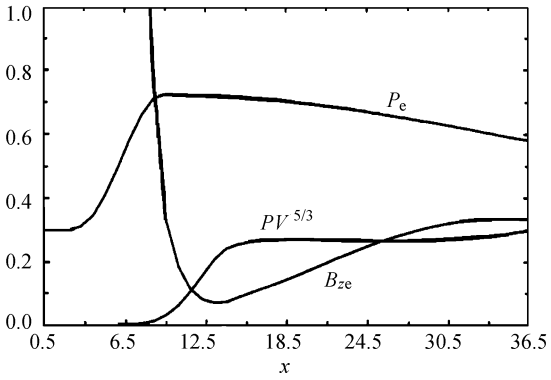

Fig. 16 Equatorial pressure P_e, entropy parameter $PV^{5/3}$, and equatorial magnetic field strength as a function of distance from Earth, as computed by a 2D equilibrium model of the magnetic field and plasma distribution. The unit of x is R_E, but the units of P_e, $PV^{5/3}$, and B_{ze} are arbitrary (From Hau[75])

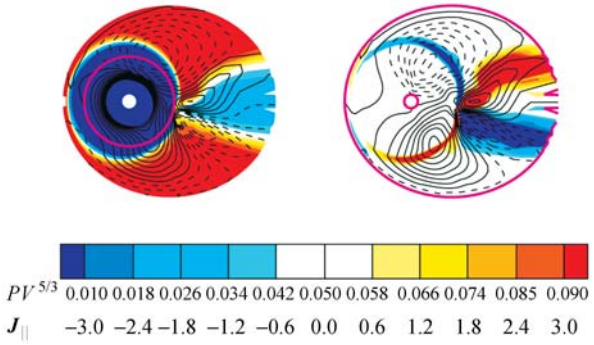

Fig. 17 Rice Convection Model simulation of the injection of a bubble in a substorm. Color in the left diagram indicates $PV^{5/3}$ in nPa$(R_E/\text{nT})^{5/3}$. In the right diagram, color indicates the density of Birkeland current in μA/m^2 down into the ionosphere, but with values mapped to the equatorial plane. Black contours indicate drift paths for an average ion (left) and equipotentials (right). The effects of induction electric fields on drift paths are not displayed, although they are considered in the calculation. Corotation is not included in the contours of the right diagram (From Zhang *et al.*[82])

carried out so far, the plasma sheet typically thins somewhat, but not to the extent observed (to about 1000 km). Equilibrium calculations have produced very thin current sheets when an additional non-adiabatic process was assumed (Lee *et al.*[70]; Yang *et al.*[72]), but the detailed physics of the non-adiabatic process is not clear yet.

Regarding the expansion phase of a substorm, observational evidence has accumulated that the dipolarized region inside the substorm current wedge is a low-$PV^{5/3}$ bubble (Lyons *et al.*[78]; Apatenkov *et al.*[79]). Our group has started to employ that idea in simulations of the earthward injection of particles in a substorm (Zhang *et al.*[80−82]; Yang[83]), and a sample result is shown in Figure 17. These calculations include the effects, on ionospheric currents and electric fields, of the Birkeland currents that necessarily flow along the sides of a bubble and form the substorm current wedge. However, attempts at realistic simulation of substorm particle injections are still in their infancy. No computational model currently exists that can include all of the physics that is obviously important to the process, including pressure-driven and inertial currents in the magnetosphere, ionosphere-magnetosphere coupling, and transport by gradient/curvature drift, all with reasonable numerical accuracy. (The Rice Convection Model (RCM) and the RCM-E, which keeps the magnetic field in equilibrium with the computed particles, in their present forms both neglect inertial currents.)

3.5 Summary Comments

It has become apparent that interchange processes in general, and bubbles in particular, play a central role in plasma-sheet transport and substorms. Still, the mechanisms for generating bubbles, which involve small-scale and large-scale processes working together to violate frozen-in-flux, are still incompletely understood. Furthermore, we do not yet have a computational framework that adequately treats the evolution of a substorm-associated bubble, once it is created.

4 Ballooning

4.1 Definition

In the classic ideal-MHD expression for the cha-

nge in the potential energy of a stationary system (Bernstein *et al.*[46]), there is a term that indicates instability if ∇P and field-line curvature are parallel to each other. Figure 18 depicts instability in a plasma device where the field-line curvature varies with distance along the magnetic field. This instability, termed "ballooning" occurs mostly in regions where the curvature is favorable for instability and the field line balloons out. The dominant modes typically have small wavelength perpendicular to $\boldsymbol{B}$.

As with magnetic reconnection theory, the theoretical study of ballooning is maddeningly complex. In common with reconnection, the physics of ballooning includes both large- and small-scale aspects: while ballooning is basically a large-scale MHD phenomenon, the ballooning growth rate is affected by small-scale kinetic effects. However, while it is clear that reconnection plays a major role in substorm dynamics, it has not yet been firmly established whether or not ballooning plays a causal role in substorms or is, instead, a minor consequence of substorms. The introduction to the paper by Zhu *et al.*[85] includes a fairly detailed review of the history of the theory of ballooning as applied to the magnetosphere, and I have based some of this brief review on material contained there.

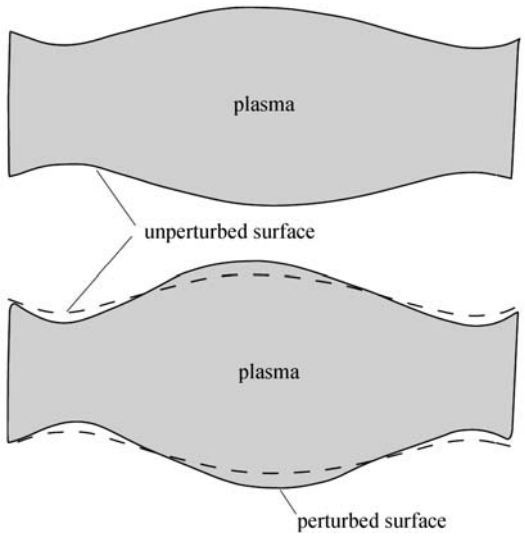

Fig. 18 Ballooning in a plasma confinement device (Adapted from Friedberg[84])

As in the case of reconnection, there is a problem with regard to definition. The confusion specifically concerns the terms "interchange instability" and "ballooning instability". Some researchers consider ballooning to be the more general term, and interchange a special case of it, characterized by situations where entire flux tubes change places. Others prefer to eliminate the distinction and combine the two using the term "ballooning/interchange". Part of the problem is in the definition of "interchange". Previously, I referred to the thin-filament motion shown in Figure 12 as an interchange process, because a filament that started life with $PV^{5/3}$ less than neighboring flux tubes moved through a medium until it found a position where the $PV^{5/3}$ of the local background matched its value. However, while the filament is evolving from its initial configuration to its final state, its shape is highly dynamic and differs from the background, and pressure is not uniform along its length.

I prefer to use the term "ballooning instability" to describe an instability that exists in ideal MHD in a situation that does not satisfy the conditions of interchange instability ((4) or (5)). As indicated in Section 3.2, the average gradients of $PV^{5/3}$ and V in the magnetosphere are both directed approximately tailward, so that the criterion for interchange instability is not satisfied in these average configurations. A crucial question, in my opinion, is whether, even under these conditions, there is still ballooning instability in the statistical-average plasma sheet or at least in the stretched plasma sheet that is characteristic of the end of the substorm growth phase.

4.2 Linear Analyses

The theoretical work of Miura *et al.*[86] suggested that Earth's plasma sheet is ballooning unstable in regions where $\beta \approx 1$. Roux *et al.*[87] found observational evidence of ripples at geosynchronous orbit in the early expansion phase of a substorm and identified those with ballooning. (See Figure 19) It is not clear whether this observed feature satisfies my definition of ballooning, since both interchange and ballooning give similar patterns of field-aligned currents. The

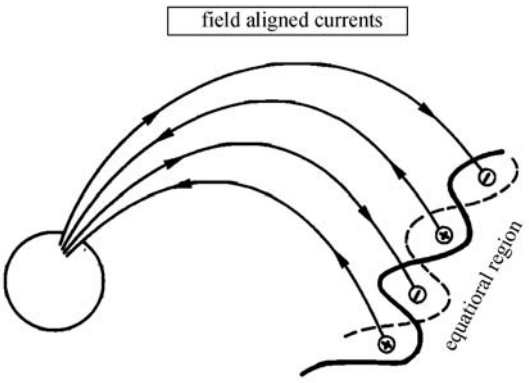

Fig. 19 Ripples with field-aligned currents of alternating signs, as observed at geosynchronous orbit (From Roux *et al.*[87])

leading edge of a bubble like the one shown on the left side of Figure 17 typically satisfies the condition of interchange instability, and interchange ripples have been seen on the leading edge of some of those bubbles in a few RCM runs done with very high resolution. From the viewpoint of the bubble injection picture, the question is whether the little ripples grow enough to be important in the few minutes it takes for the bubble to reach the inner magnetosphere. Of course, little interchange ripples on the leading edge of an earthward-rushing bubble are a by-product of the bubble and not a primary driver.

Lee and Wolf[88] applied the classic Bernstein energy principle to a set of analytic 2D equilibrium models of the plasma-sheet and found that most configurations were stable against ballooning if they were stable against interchange, though some were extremely close to the threshold of ballooning instability. The situation is complicated by the fact that the ionospheric ends of plasma-sheet field lines are effectively closed so that compressibility of the plasma has a significant effect. Ohtani and Tamao[89], Lee and Min[90], and Schindler and Birn[91] reached similar conclusions. However, Lee[92], Bhattacharjee *et al.*[93], Cheng and Lui[94], Cheng[95] and Cheng and Zaharia[96] found highly stretched (mostly numerical) equilibria in which ballooning instability seems to occur near the inner edge of the plasma sheet. The abovementioned analyses have all been essentially 1D, employing the assumption that variations along the magnetic field have much longer length scales than variations perpendicular to $\boldsymbol{B}$. (This so-called $k_y \to \infty$ approximation lends itself to analytic treatment.) However, Wu *et al.*[97] and Zhu *et al.*[98] used 2D MHD for linear analyses of ballooning instability, including finite k_y. Some theorists have treated ballooning instability using formalisms that are more high-powered than ideal MHD: Pu *et al.*[99], Lee[100], and Zhu *et al.*[101] utilized drift and Hall MHD, and Cheng and Lui[94], Wong *et al.*[102], and Crabtree *et al.*[103] used gyrokinetic treatments. The majority of the recent studies seem to agree that the plasma sheet is frequently unstable to ballooning, and that the most unstable region lies in the inner plasma sheet, where $\beta \approx 1$. Highly stretched configurations with thin current sheets also tend to be more unstable than configurations in which the plasma sheet is more dipole-like (Zhu *et al.*[98,101]).

4.3 Nonlinear Development

Given the likelihood of linear instability, the question is whether ballooning can grow fast enough to cause something with the explosive evolution of a substorm onset. It has been suggested that the nonlinear evolution of ballooning of the inner plasma sheet accelerates into a "detonation" event. (See Hurricane *et al.*[104] and references therein.) However, Zhu *et al.*[85] used a 3D MHD simulation to study the nonlinear evolution of a plasma-sheet-like configuration that is linearly unstable to ballooning. They started with an equilibrium that included a 2D dipole and a tail in which the stretching could be adjusted. They found that initial perturbations grew exponentially but then saturated, as shown in Figure 20, with no major disruption of the current sheet.

Other simulations have suggested that the nonlinear evolution of ballooning may not be explosive. While Pritchett and Coroniti[105] found a ballooning instability in their PIC code during driven reconnection, it did not result in any change in magnetic topology. Zhu *et al.*[106] investigated substorm ballooning

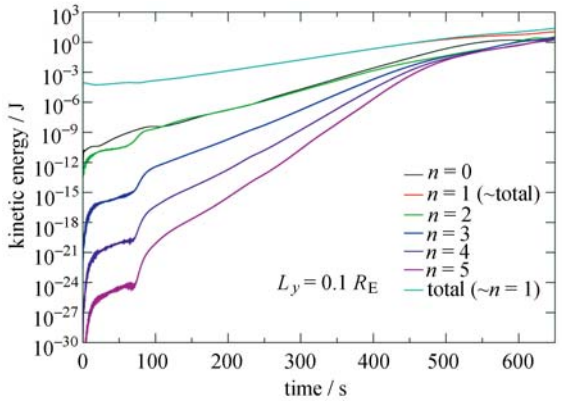

Fig. 20 Growth of the kinetic energy in different Fourier components of a ballooning disturbance (*i.e.*, different k_p). From Zhu *et al.*[85]

using configurations computed by the OpenGGCM global MHD code and found that the instability criterion was satisfied in the late growth phase of a THEMIS-observed substorm of March 23, 2007. While the code did show some evidence of ballooning around onset, when reconnection started and proceeded rapidly, it was not clear that ballooning was involved in initiating the reconnection. Raeder *et al.*[107] have tentatively described the disturbance that preceded reconnection in the March 2007 substorm as "$k_y = 0$ ballooning", but that mode seems quite different from ordinary ballooning, and its physical nature is not yet clear.

4.4 Concluding Comments on Ballooning

It should be remarked that papers dealing with ballooning theory do not normally include plots of $PV^{5/3}$, which is the key parameter for deciding on whether a configuration is interchange unstable. Thus some of the balloon-unstable configurations described by the papers cited in Section 4.2 may also be interchange unstable.

To summarize the present situation, the majority of experts agree that the inner plasma sheet is frequently linearly unstable to ballooning, but it is still not clear that ballooning instability plays a crucial role in substorm onset.

5 3D Global MHD Models

5.1 Introductory Comments

Until now I have dealt with specific physical processes that play (or at least may well play) major roles in substorms. These processes have been investigated using different forms of analytic theory and various kinds of simulations. In the present section I turn my attention to work done with one specific type of simulation that attempts to represent all of the large-scale aspects of substorms (and other magnetospheric phenomena) in a single computational framework by parameterizing (or ignoring) the smaller-scale processes.

Leboeuf *et al.*[108], Brecht *et al.*[109], and Wu *et al.*[110] reported the first results from 3d global MHD simulations of the magnetosphere. A huge amount of work has been poured into this type of code in the last 30 years. Helped along by the dramatic increase in available computing power, these codes have evolved from amusing toys to tools that are indispensible to the scientific community. The model utilized by Brecht *et al.*[109], which had its roots in a code developed for U. S. defense work, evolved into the what is now called the Lyon-Fedder-Mulberry (LFM) code (Lyon *et al.*[111]). Another of the present leading global-simulation codes originated in the early 1990s (Raeder[112]) and is now called OpenGGCM (Raeder *et al.*[113]). The BATSRUS (Block-Adaptive-Tree Solar-wind Roe-type Upwind Scheme) code is of more recent design and utilizes adaptive-grid technology (Powell *et al.*[114]). Several other 3D global MHD codes have been developed and have proved quite useful (Ogino *et al.*[115]; Palmroth *et al.*[116]; White *et al.*[117]; Winglee *et al.*[118]). The various global MHD codes differ principally in their choice of numerical method and grid. Versions of the most popular codes are available at the Community Coordinated Modeling Center (ccmc.gsfc.nasa.gov), where huge libraries of past run results can be viewed, and users can request runs on demand. Thousands of such runs have

been completed at the request of scores of users, for a wide variety of purposes.

The outer boundary of the modeling region for these codes is usually set well out in the solar wind, and the primary inputs are the density, velocity, and magnetic field in the solar wind. The inner boundary is typically placed at about $2{\sim}3\,R_{\rm E}$. Birkeland currents are usually mapped down to the ionosphere assuming a dipole magnetic field, where the current conservation equation

$$\nabla \cdot (\Sigma \cdot \nabla \Phi) = -J_{\parallel}$$

is solved for the ionospheric potential Φ. Here Σ is the ionospheric conductance tensor, and Φ is the electric potential. The potential is mapped back to the MHD inner boundary to provide the boundary condition on the plasma velocity parallel to the boundary. A variety of conductance models have been used, but most contain representations of the conductance due to sunlight and some rough estimate of the diffuse aurora. The conductance is additionally enhanced in regions where the MHD code predicts upward current.

5.2 Sample Results for Substorms

The global-MHD models get many general characteristics of substorms qualitatively right. A period of southward IMF results in storage of energy in the tail of the model magnetosphere. There is often a sudden release of stored energy and associated dipolarization of some plasma-sheet field lines, and there is injection of fresh plasma into the geosynchronous region. Thus the models are sufficiently realistic to serve as a baseline for observers, and the biggest use of the models, to date, has been in modeling real events, helping observers interpret aspects of their measurements.

Figure 21 shows a sample result from an early effort to simulate a magnetospheric substorm. The figure compares the observed large-scale auroral pattern from the Viking satellite to a synthetic image constructed from the model-computed precipitating

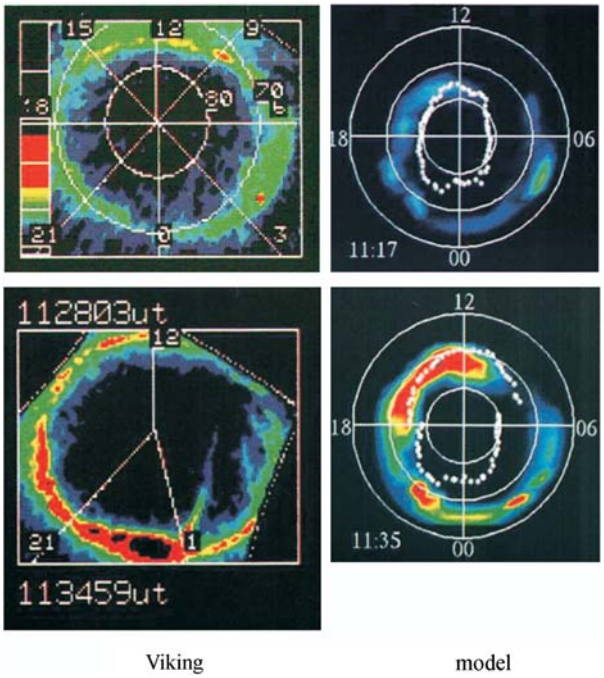

Fig. 21 Comparison of auroral patterns observed from the LBH image taken from the Viking spacecraft, which is indicative of total precipitating energy flux, with a synthetic image computed from the precipitating energy flux estimated from the MHD simulation. The upper plots are for a time before onset, while the lower ones are for a time near the peak of the substorm expansion. The open-closed boundary is indicated by white stars in the model plot (Adapted from Fedder *et al.*[119])

electron energy flux. The bright aurora in the synthetic image correspond to regions of upward Birkeland current, which tend to result in electric fields upward along the field lines, which accelerate electrons downward. The color scale in the model plots is not identical to the observational scale, but, rather, was chosen to emphasize comparable features.

Wiltberger *et al.*[120] carried out a more detailed computational study and analysis of a magnetospheric substorm, using a later version of the same LFM code. Figure 22 shows a sample comparison of computed plasma and magnetic field values with observations from two different spacecraft that were in the magnetotail during the event.

Figure 23 presents results from an even more ambitious comparison, this time between the OpenGG-

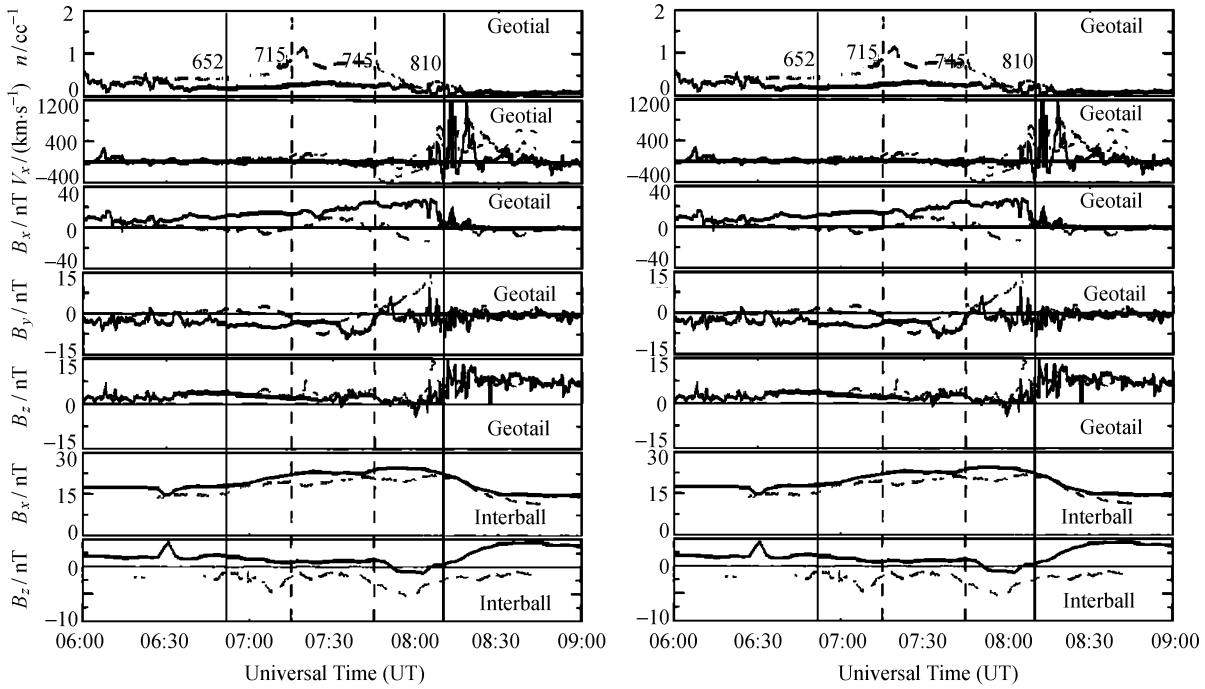

Fig. 22 Comparison of LFM model results (dashed curves) with measurements from Geotail and Interball spacecraft. Geotail was at about ($x = -19.8$, $y = 8$, $z = -1$), and Interball was at about ($x = -25$, $y = 10$, $z = 8$). The first solid vertical line marks the beginning of the growth phase. The first dashed line represents a small release of lobe field energy, while the second dashed line represents the start of tailward flow at Geotail in the simulation. The final solid line represents a dipolarization at the geosynchronous spacecraft GOES 9 (From Wiltberger *et al.*[120])

CM MHD code and observations, for the GEM Substorm Challenge event of November 24, 1996. The IMF turned southward at about 21:00 UT, and the modeled AL index reached its maximum absolute value at about 22:30 UT. Model predictions are compared with corresponding patterns computed from AMIE (Assimilative Mapping of Ionospheric Electrodynamics), which assimilated data from Super DARN coherent backscatter radar sites and a large suite of ground magnetometers, to find a best-fit representation of the ionospheric-potential and Birkeland-current patterns.

Although the primary effort in applying global MHD codes to investigate substorms has been in the area of event simulations and direct comparisons with observations, the models have also been used to investigate specific physical questions. One interesting example is an attempt to answer the most central question of substorm physics, namely, why energy gets stored in the tail lobes to be released in the expansion phase, which has a sudden onset. Siscoe *et al.*[122] pointed out that a similar buildup/sudden-release phenomenon occurs in coronal mass ejections. They noted that global MHD simulations of Earth's magnetosphere indicate that, after energy is stored in the tail, reconnection inside the inner plasma sheet is preceded by a departure from force balance and accompanying accelerating flows. In two sequel papers, Zhu *et al.*[106] and Raeder *et al.*[107] applied the criterion for ballooning instability to determine whether the departure from force balance resulted from ballooning instability; they found evidence for conventional large-k_y ballooning in the simulation results, but that ballooning does not appear to be the source of the force imbalance and subsequent reconnection. Based on detailed examination of the simulation resu-

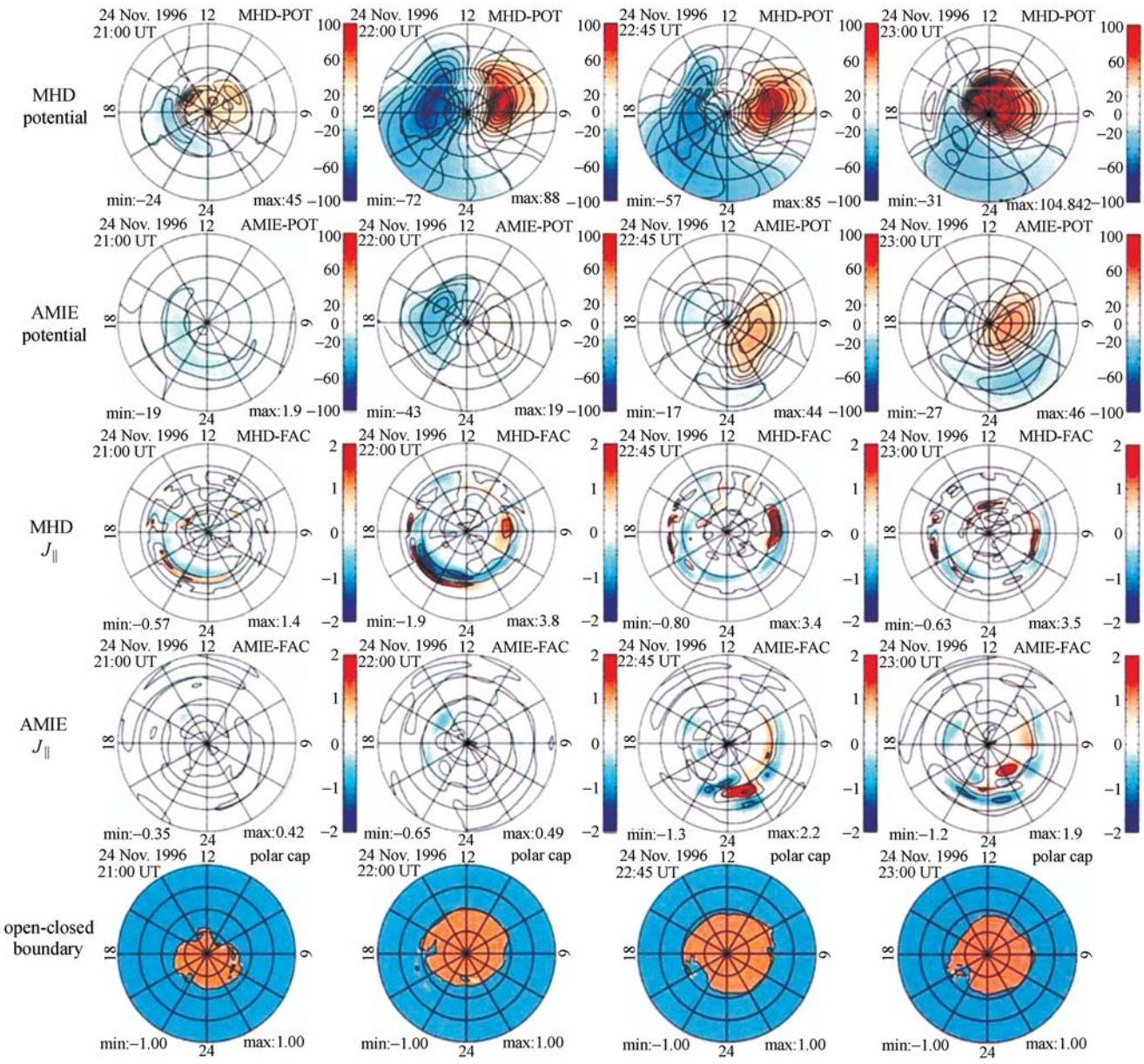

Fig. 23 Comparison of ionospheric potentials and Birkeland current densities computed by the first-principles OpenGGCM MHD model with those calculated from ground-magnetometer and coherent-backscatter radar data by the AMIE procedure. Positive field-aligned currents are down (From Raeder *et al.*[121])

lts, Raeder *et al.*[107] have suggested that the force imbalance instead results from a ballooning-type disturbance that has a long length scale in the y-direction, which they call a KY0 mode. Yang *et al.*[72] have suggested a different interpretation that is based on an interchange effect, and they have found evidence for it in OpenGGCM simulations (Hu *et al.*[123]). While this issue is still far from being settled, it is an example of how global MHD simulations may eventually prove very useful in answering fundamental questions about substorms.

As indicated in Figures 20–22, while straight comparisons of global MHD simulations with substorm observations indicate a general tendency toward agreement, there is nothing close to the detailed agreement that would convince the casual observer

that the model was really locked into the physics of the phenomenon. There are several possible reasons for the disagreements.

(1) The model may not properly represent the effects of small-scale plasma phenomena on large-scale dynamics.

(2) The models do not always do an accurate job of solving the ideal MHD equations (more on this later).

(3) The solar-wind inputs to the models, which are usually derived from spacecraft hundreds of $R_{\rm E}$ upstream from the Earth, may not be representative of what actually hits the bow shock.

(4) The magnetosphere has a number of sharp boundaries that involve large spatial gradients and move in time; if the model is slightly off in its prediction of the location of the boundary, that may cause its predictions of plasma and magnetic field parameters to be very inaccurate at a specific spacecraft locations.

5.3 Limitations

Given their wide use in the community, it is important to remember that global MHD models have important limitations, including the following.

(1) Global MHD results often depend on grid spacing. Because they cover an enormous region of space (hundreds of thousands of $R_{\rm E}^3$) and magnetospheric boundaries are often quite sharp, the results are grid-limited, and the codes tend to make structures look fuzzier than they really are. Grid resolution problems are especially acute in the representation of ionosphere-magnetosphere coupling. Auroral Birkeland currents and potentials are mapped between the ionosphere and an MHD inner boundary at about $3\,R_{\rm E}$. The auroral zone typically occupies a relatively small number of grid points on the $3\,R_{\rm E}$ boundary, which severely limits accuracy. (The numerical accuracy of global MHD models has been discussed by Ridley *et al.*[124])

(2) Most (but not all) simulation runs assume ideal MHD, which, as noted earlier, precludes reconnection, which is the dominant mechanism that feeds energy from the solar wind to the magnetosphere. Thus the interesting results from the codes are usually consequences of numerical error and are based on the assumption that either the results are insensitive to the amount of dissipation or that numerical error in the codes adequately mimics the dissipation that in Nature results from small-scale plasma processes.

(3) Ideal MHD does not include transport by gradient/curvature drift, which is very important in the ring current region. This problem has been addressed by coupling inner-magnetosphere-drift models to MHD codes, but that effort has not gone smoothly. Several one-way couplings have been accomplished using different combinations of MHD and inner-magnetosphere codes (*e.g.*, Toffoletto *et al.*[125]; Keller *et al.*[126]; Hu *et al.*[123]), but two-way-coupled runs, in which the inner-magnetosphere model corrects MHD-computed pressures and densities, are still tricky and have reached publishable form only for the coupling of BATS-R-US and RCM (*e.g.*, DeZeeuw *et al.*[127]; Zhang *et al.*[128]).

(4) The arguments presented in Section 3 indicate that $PV^{5/3}$ plays a crucial role in plasma-sheet dynamics. It should be conserved in slow-flow ideal MHD, and the parameter $\left[\int P^{3/5}{\rm d}s/B\right]^{5/3}$ should be conserved even with fast-flow MHD, providing that there are no shock waves. However, global MHD codes do not always conserve these quantities accurately in the plasma sheet, due to numerical diffusion.

(5) Often, results from global MHD codes are sufficiently complex that they are hard to interpret physically.

Returning to the analogy pictured in Figure 1, the island representing the accomplishments of global MHD is large. However, it is also marshy, and it is difficult to traverse long distances on that island without getting stuck in the mud.

6 Overall Summary

In the terms of Figure 1, substorm observers and

data analysts have frequently swum to theoretical islands and adopted ideas from them. In most cases, the theoretical islands are based on ideas that were originally developed for other areas of plasma physics (solar physics, laboratory plasmas). Theorists' work to expand and solidify the islands has been of significant help in interpreting observations. Thus, even though theorists have rarely been at the center of substorm physics, they have often helped observers avoid drowning in their data. However, even after decades of work, the theoretical islands are all either small or dangerous, as all of the theories and simulations have serious limitations.

Acknowledgements The author is grateful to Bob Spiro for careful reading and skillful editing of the manuscript. The author also thanks Frank Toffoletto for helpful comments and Jack Gosling for contributing a figure.

References

[1] Schwarzschild B. Enormous reconnection event washes over three spacecraft millions of kilometers apart [J]. *Phys. Today*, 2006, **59**(3):18-22

[2] Paschmann G. Space physics: Breaking through the lines [J]. *Nature*, 2006, **439**(7073):144-145

[3] Giovanelli R G. A theory of chromospheric flares [J]. *Nature*, 1946, **158**(4003):81-82

[4] Hoyle F. Some Recent Researches in Solar Physics [M]. Cambridge: Cambridge University Press, 1949

[5] Dungey J W. Conditions for occurrence of electrical discharges in astrophysical systems [J]. *Phil. Mag.*, 1953, **44**(354): 725-738

[6] Furth H I, Killeen J, Rosenbluth M N. Finite-resistivity instabilities in a sheet pinch [J]. *Phys. Fluids*, 1963, **6**(4): 459-484

[7] Siscoe G L. Solar system magnetohydrodynamics [M]// Carovillano R L, Forbes J M. Solar-Terrestrial Physics. Dordrecht-Holland; D. Reidel Publ. Co. 1983. 11-100

[8] Sweet P A. The neutral point theory of solar flares [M]//Lehnert B ed. Electromagnetic Phenomena in Cosmical Physics. London: Cambridge University Press. 1958. 123-134

[9] Parker E N. Sweet's mechanism for merging magnetic fields in conducting fluids [J]. *J. Geophys. Res.*, 1957, **62**(4):509-520

[10] Petschek H E. Magnetic field annihilation [C]//Proceedings of the AAS-NASA Symposium on the Physics of Solar Flares, NASA Spec Publ SP-50, F, 1964, NASA

[11] Vasyliunas V M. Theoretical models of magnetic field-line merging, 1 [J]. *Rev. Geophys. Space Phys.*, 1975, **13**(1): 303-336

[12] Dungey J W. Interplanetary magnetic field and the auroral zones [J]. *Phys. Rev. Lett.*, 1961, **6**(2):47-48

[13] Coppi B, Laval G, Pellat R. Dynamics of the geomagnetic tail [J]. *Phys. Rev. Lett.*, 1966, **16**(26):1207-1208

[14] Russell C T, McPherron R L. The magnetotail and substorms [J]. *Space Sci. Rev.*, 1973, **15**(2-3):205-266

[15] McPherron R L, Russell C T, Aubry M P. Satellite studies of magnetospheric substorms on August 15, 1968, 9. Phenomenological model for substorms [J]. *J. Geophys. Res.*, 1973, **78**(16):3131-3149

[16] Birn J, Drake J F, Shay M A, Rogers B N, Denton R E, Hesse M, Kuznetsova M, Ma Z W, Bhattacharjee A, Otto A, Pritchett P L. Geospace Enviornmental Modeling (GEM) magnetic reconnection challenge [J]. *J. Geophys. Res.*, 2001, **106**(A3):3715-3719

[17] Otto A. Geospace Environment Modeling (GEM) magnetic reconnection challenge: MHD and Hall MHD-constant and current dependent resistivity models [J]. *J. Geophys. Res.*, 2001, **106** (A3):3751-3758

[18] Shay M A, Drake J F, Rogers B N, Denton R E. Alfvénic collisionless magnetic reconnection and the Hall term [J]. *J. Geophys. Res.*, 2001, **106**(A3):3759-3772

[19] Hesse M, Birn J, Kuznetsova M. Collisionless magnetic reconnection: Electron processes and transport modeling [J]. *J. Geophys. Res.*, 2001, **106**(A3): 3721-3735

[20] Asano Y, Mukai T, Hoshino M, Saito Y, Hayakawa H, Nagai T. Current sheet structure around the near-Earth neutral line observed by Geotail [J]. *J. Geophys. Res.*, 2004, **109**(A2): A022212, doi: 10.1029/2003JA010114

[21] Hesse M, Zenitani S, Kuznetsova M M, Birn J. Multiscale physics in the magnetosphere: The role of magnetic reconnection [M]. Abstract SM33E-05 presented at 2010 Fall Meeting AGU, San Francisco, 2010

[22] Gosling J T, Phan T D, Lin R P, Szabo A. Prevalence of magnetic reconnection at small field shear angles in the solar wind [J]. *Geophys. Res. Lett.*, 2007, **34**(15):L15110, doi: 10.1029/2007gl030706

[23] Schindler K, Hesse M, Birn J. General magnetic reconnection, parallel electric fields, and helicity [J]. *J. Geophys. Res.*, 1988, **93**(A6):5547-5557

[24] Axford W I. Magnetic field reconnection [M]//Hones E W ed. Magnetic Reconnection in Space and Laboratory Plasmas, Washington D C: America Geophys. Un.,1984. 1-8

[25] Hesse M, Schindler K. A theoretical foundation of general magnetic reconnection [J]. *J. Geophys. Res.*, 1988, **93**(A6):5559-5567

[26] Hesse M, Schindler K, Birn J, Kuznetsov E. The diffusion region in collisionless magnetic reconnection [J]. *Phys.*

Plasmas, 1999, **6**(5):1781-1795

[27] Pritchett P L, Coroniti F V. Three-dimensional collisionless magnetic reconnection in the presence of a guide field [J]. *J. Geophys. Res.*, 2004, **109**(A1): A01220, doi: 10.1029/2003JA009999

[28] Hesse M, Birn J. On dipolarization and its relation to the substorm current wedge [J]. *J. Geophys. Res.*, 1991, **96**(A11):19 417-19 426

[29] Birn J, Hesse M. Details of current disruption and diversion in simulations of magnetotail dynamics [J]. *J. Geophys. Res.*, 1996, **101**(A7):15 345-15 358

[30] Birn J, Hesse M, Schindler K. Formation of thin current sheets in space plasmas [J]. *J. Geophys. Res.*, 1998, **103**(A4):6843-6852

[31] Birn J, Schindler K, Hesse M. Formation of thin current sheets in the magnetotail: Effects of propagating boundary deformations [J]. *J. Geophys. Res.*, 2003, **108**(A9): 1337, doi: 10.1029/2002JA009641

[32] Birn J, Hesse M, Schindler K, Zaharia S. Role of entropy in magnetotail dynamics [J]. *J. Geophys. Res.*, 2009, **114**(d): A00d03, doi 10.1029/2008ja014015

[33] Schindler K. A theory of the substorm mechanism [J]. *J. Geophys. Res.*, 1974, **79**(19):2803-2810

[34] Galeev A A, Zelenyi L M. Tearing instability in plasma configurations [J]. *JETP*, 1976, **43**(6):2133-2151

[35] Lembège B, Pellat R. Stability of a thick two-dimensional quasi-neutral sheet [J]. *Phys. Fluids*, 1982, **25**(11):1995-2004

[36] Pellat R, Coroniti F V, Pritchett P L. Does ion tearing exist? [J]. *Geophys. Res. Lett.*, 1991, **18**(2):143-146

[37] Brittnacher M, Quest K B, Karimabadi H. On the energy principle and ion tearing in the magnetotail [J]. *Geophys. Res. Lett.*, 1994, **21**(15):1591-1594

[38] Quest K B, Karimabadi H, Brittnacher M. Consequences of particle conservation along a flux surface of magnetotail tearing [J]. *J. Geophys. Res.*, 1996, **101**(A1):179-183

[39] Schindler K. Physics of Space Plasma Activity [M]. Cambridge: Cambridge University Press, 2007

[40] Sitnov M I, Schindler K. Tearing stability of a multiscale magnetotail current sheet [J]. *Geophys. Res. Lett.*, 2010, **37**(8):L08102, doi: 10.01029/2010GL042961

[41] Pritchett P L. Collisionless magnetic reconnection in a three-dimensional open system [J]. *J. Geophys. Res.*, 2001, **106**(A11):25 961-25 977

[42] Pritchett P L. Externally driven magnetic reconnection in the presence of a normal magnetic field [J]. *J. Geophys. Res.*, 2005, **110**(A5), A05209, doi: 10.1029/2004JA010948

[43] Rosenbluth M N, Longmire C L. Stability of plasmas confined by magnetic fields [J]. *Ann. Phys.*, 1957, **1**(2):120-140

[44] Sonnerup B U Ö, Laird M J. On the magnetospheric interchange instability [J]. *J. Geophys. Res.*, 1963, **68**(1):131-138

[45] Schmidt G. Physics of High Temperature Plasmas, 2nd edition [M]. New York: Academic Press, 1979

[46] Bernstein I B, Frieman E A, Kruskal M D, Kulsrud R M. An energy principle for hydromagnetic stability problems [J]. *Proc. Royal. Soc. London*, 1958, **A244**(1236): 17-40

[47] Xing X, Wolf R A. Criterion for interchange instability in a plasma connected to a conducting ionosphere [J]. *J. Geophys. Res.* 2007, **112**(12), A12209, doi: 10.1029/2007JA012535

[48] Erickson G M, Wolf R A. Is steady convection possible in the Earth's magnetotail [J]. *Geophys. Res. Lett.*, 1980, **7**(11):897-900

[49] Kaufmann R L, Paterson W R, Frank L A. Pressure, volume, and density relationships in the plasma sheet [J]. *J. Geophys. Res.*, 2004, **109**(A8), A08204, doi: 10.1029/2003JA010317

[50] Baumjohann W, Paschmann G, Cattell C A. Average plasma properties in the central plasma sheet [J]. *J. Geophys. Res.*, 1989, **94**(A6):6597-6606

[51] Tsyganenko N A. On the convective mechanism for formation of the plasma sheet in the magnetospheric tail [J]. *Planet Space. Sci.*, 1982, **30**(10):1007-1012

[52] Spence H E, Kivelson M. Contributions of the low-latitude boundary layer to the finite width magnetotail convection model [J]. *J. Geophys. Res.*, 1993, **98**(A9):15 487-15 496

[53] Wang C P, Lyons L R, Chen M W, Toffoletto F R. Modeling the transition of the inner plasma sheet from weak to enhanced convection [J]. *J. Geophys. Res.*, 2004, **109**(A12), A12202, doi:10.1029/2004JA010591

[54] Pontius D H Jr, Wolf R A. Transient flux tubes in the terrestrial magnetosphere [J]. *Geophys. Res. Lett.*, 1990, **17**(1):49-52

[55] Baumjohann W, Paschmann G, Lühr H. Characteristics of high-speed ion flows in the plasma sheet [J]. *J. Geophys. Res.*, 1990, **95**(A4):3801-3809

[56] Angelopoulos V, Baumjohann W, Kennel C F, Coroniti F V, Kivelson M G, Pellat R, Walker R J, Lühr H, Paschmann G. Bursty bulk flows in the inner central plasma sheet [J]. *J. Geophys. Res.*, 1992, **97**(A4):4027-4039

[57] Angelopoulos V. Transport Phenomena in the Earth's Plasma Sheet [D]. UCLA, 1993

[58] Chen C X, Wolf R A. Interpretation of high speed flows in the plasma sheet [J]. *J. Geophys. Res.*, 1993, **98**(A12):21 409-21 419

[59] Sergeev V A, Angelopoulos V, Gosling J T, Cattell C A, Russell C T. Detection of localized, plasma-depleted flux tubes or bubbles in the midtail plasma sheet [J]. *J. Geophys. Res.*, 1996, **101**(A5):10 817-10 826

[60] Kauristie K, Sergeev V A, Kubyshkina M, Pulkkinen T I, Angelopoulos V, Phan T, Lin R P, Slavin J A. Ionospheric current signatures of transient plasma sheet flows [J]. *J.*

Geophys. Res., 2000, **105**(A5):10 677-10 690

[61] Nakamura R, Baumjohann W, Schodel R, Brittnacher M, Sergeev V A, Kubyshkina M, Mukai T, Liou K. Earthward flow bursts, auroral streamers, and small expansions [J]. *J. Geophys. Res.*, 2001, **106**(A6):10 791-10 802

[62] Chen C X, Wolf R A. Theory of thin-filament motion in Earth's magnetotail and its application to bursty bulk flows [J]. *J. Geophys. Res.*, 1999, **104**(A7):14 613-14 626

[63] Panov E V, Nakamura R, Baumjohann W, Angelopoulos V, Petrukovich A A, Retino A, Volwerk M, Takada T, Glassmeier K H, Mcfadden J, Larson D. Multiple overshoot and rebound of a bursty bulk flow [J]. *Geophys. Res. Lett.*, 2010, **37**(8):L0810310, doi:10.1029/2009GL0141971

[64] Birn J, Raeder J, Wang Y L, Wolf R A, Hesse M. On the propagation of bubbles in the geomagnetic tail [J]. *Ann. Geophys.*, 2004, **22**(5):1773-1786

[65] Birn J, Nakamura R, Panov E V, Hesse M. Bursty bulk flows and dipolarization in MHD simulations of magnetotail reconnection [J]. *J. Geophys. Res.*, 2011 (in press)

[66] Pritchett P L, Coroniti F V. A kinetic ballooning/interchange instability in the magnetotail [J]. *J. Geophys. Res.*, 2010, **115**(A6), A06301, doi:10.1029/2009JA-014752

[67] Sitnov M I, Swisdak M, Divin A V. Dipolarization fronts as a signature of transient reconnection in the magnetotail [J]. *J. Geophys. Res.*, 2009, **114**(A4):A04202, 10.1029/2008ja013980

[68] Runov A, Angelopoulos V, Sitnov M, Sergeev V A, Nakamura R, Nishimura Y, Frey H U, Mcfadden J P, Larson D, Bonnell J, Glassmeier K-H, Auster U, Conners M, Russell C T, Singer H J. Dipolarization fronts in the magnetotail plasma sheet [J]. *Planet Space Sci.*, 2011 (in press)

[69] Lui A T Y. Magnetospheric substorms [J]. *Phys. Fluids: B*, 1992, **4**(7):2257-2263

[70] Lee L C, Zhang L, Choe G S, Cai H J. Formation of a very thin current sheet in the near-Earth magnetotail and the explosive growth phase of substorms [J]. *Geophys. Res. Lett.*, 1995, **22**(9):1137-1140

[71] Lee L C, Zhang L, Otto A, Choe G S, Cai H J. Entropy antidiffusion instability and formation of a thin current sheet during geomagnetic substorms [J]. *J. Geophys. Res.*, 1998, **103**(A12):29 419-29 428

[72] Yang J, Wolf R A, Toffoletto F R. RCM-E simulation results of accelerated thinning of the near-Earth plasma sheet caused by a bubble-blob pair [J]. *Geohys. Res. Lett.*, 2011, (in press)

[73] Wolf R A, Wan Y, Xing X, Zhang J-C, Sazykin S. Entropy and plasma sheet transport [J]. *J. Geophys. Res.*, 2009, **114**(A0):A00D05, doi:10.1029/2009JA014044

[74] Erickson G M. Modeling of plasma-sheet convection: implications for substorms [D]. Houston T X:Rice University, 1985

[75] Hau L-N. Effect of steady-state adiabatic convection on the configuration of the near-Earth plasma sheet, 2 [J]. *J. Geophys. Res.*, 1991, **96**(A4):5591-5596

[76] Toffoletto F R, Spiro R W, Wolf R A, Hesse M, Birn J. Self-consistent modeling of inner magnetospheric convection [R]//Rolfe E J, Kaldeich B. Proc Third International Conference on Substorms (ICS-3), ESA SP-389. Noordwijk, The Netherlands; ESA Publications Division, 1996. 223-230

[77] Lemon C, Wolf R A, Hill T W, Sazykin S, Spiro R W, Toffoletto F R, Birn J, Hesse M. Magnetic storm ring current injection modeled with the Rice Convection Model and a self-consistent magnetic field [J]. *Geophys. Res. Lett.*, 2004, **31**(21):L21801, doi:10.1029/2004GL020914

[78] Lyons L R, Wang C-P, Nagai T, Mukai T, Saito Y, Samson J C. Substorm inner plasma sheet particle reduction [J]. *J. Geophys. Res.*, 2003, **108**(A12):426, doi:10.1029/2003JA-010177

[79] Apatenkov S V, Sergeev V A, Kubyshkina M V, Nakamura R, Baumjohann W, Runov A, Alexeev I, Fazakerley A, Frey H, Muhlbachler S, Daly P W, Sauvaud J A, Ganushkina N, Pulkkinen T, Reeves G D, Khotyaintsev Y. Multi-spacecraft observation of plasma dipolarization/injection in the inner magnetosphere [J]. *Ann. Geophys.*, 2007, **25**(3):801-814

[80] Zhang J-C, Wolf R A, Sazykin S, Toffoletto F R. Injection of a bubble into the inner magnetosphere [J]. *Geophys. Res. Lett.*, 2008, **35**(2):L02110, doi:10.1029/2007GL-032048

[81] Zhang J-C, Wolf R A, Erickson G M, Spiro R W, Toffoletto F R, Yang J. Rice Convection Model simulation of the injection of an observed bubble into the inner magnetosphere:1. Magnetic-field and other inputs [J]. *J. Geophys. Res.* 2009, **114**(A8):A08218, doi:10.1029/2009JA-01430

[82] Zhang J-C, Wolf R A, Spiro R W, Erickson G M, Sazykin S, Toffoletto F R, Yang J. Rice Convection Model simulation of the injection of an observed bubble into the inner magnetosphere:2. Simulation results [J]. *J. Geophys. Res.*, 2009, **114**(8):A08219, doi:10.1029/2009JA014131

[83] Yang J. Inner Magnetospheric Modeling During Geomagnetic Active Times [D]. Houston T X: Rice University, 2009

[84] Friedberg J P. Ideal Magnetohydrodynamics [M]. New York: Plenum Press, 1987

[85] Zhu P, Sovinec C R, Hegna C C, Bhattacharjee A, Germaschewski K. Nonlinear ballooning instability in the near-Earth magnetotail: Growth, structure, and possible role in substorms [J]. *J. Geophys. Res.*, 2007, **112**(A6):A06222, doi: 10.1029/2006JA011991

[86] Miura A, Ohtani S, Tamao T. Ballooning instability and structure of diamagnetic hydromagnetic waves in a model magnetosphere [J]. *J. Geophys. Res.*, 1989, **94**(A11):15 231-15 242

[87] Roux A, Perraut S, Robert P, Morane A, Pedersen A, Korth A, Kremser G, Aparicio B, Rodgers D, Pellinen R. Plasma sheet instability related to the westward traveling surge [J]. *J. Geophys. Res.*, 1991, **96**(A10):17 697-17 714

[88] Lee D-Y, Wolf R A. Is the earth's magnetotail balloon unstable [J]. *J. Geophys. Res.*, 1992, **97**(A12):19 251-19 257

[89] Ohtani S-I, Tamao T. Does the ballooning instability trigger substorms in the near-earth magnetotail [J]. *J. Geophys. Res.*, 1993, **98**(A11):19 369-19 379

[90] Lee D-Y, Min K W. On the possibility of the MHD-ballooning instability in the magnetotail-like field reversal [J]. *J. Geophys. Res.*, 1996, **101**(A8):17 347-17 354

[91] Schindler K, Birn J. MHD stability of magnetotail equilibria including a background pressure [J]. *J. Geophys. Res.*, 2004, **109**(A10), A10208, doi:10.1029/2004JA010537

[92] Lee D-Y. Ballooning instability in the tail plasma sheet [J]. *Geophys. Res. Lett.*, 1998, **25**(21):4095-4098

[93] Bhattacharjee A, Ma Z W, Wang X. Ballooning instability of a thin current sheet in the high-Lundquist-number magnetotail [J]. *Geophys. Res. Lett.*, 1998, **25**(6):861-864

[94] Cheng C Z, Lui A T Y. Kinetic ballooning instability for substorm onset and current disruption observed by AMPTE/CCE [J]. *Geophys. Res. Lett.*, 1998, **25**(21):4091-4094

[95] Cheng C Z. Physics of substorm growth phase, onset, and dipolarization [J]. *Space Sci. Rev.*, 2004, **113**(1-2):207-270

[96] Cheng C Z, Zaharia S. MHD ballooning instability in the plasma sheet [J]. *Geophys. Res. Lett.*, 2004, **31**(6), L06809, 10.01029/2003GL018823

[97] Wu C-C, Pritchett P L, Coroniti F V. Hydromagnetic equilibrium and instabilities in the convectively driven near-Earth plasma sheet [J]. *J. Geophys. Res.*, 1998, **103**(A6):11 797-11 801

[98] Zhu P, Bhattacharjee A, Ma Z W. Finite $k(y)$ ballooning instability in the near-Earth magnetotail [J]. *J. Geophys. Res.*, 2004, **109**(A11):A11211, doi:10.1029/12004JA-010505

[99] Pu Z Y, Korth A, Chen Z X, Friedel R H W, Zong Q C, Wang X M, Hong M H, Fu S Y, Liu Z X, Pulkkinen T I. MHD drift-ballooning instability near the inner edge of the near-Earth plasma sheet and its application to substorm onset [J]. *J. Geophys. Res.*, 1997, **102**(A7):14 397-14 406

[100] Lee D-Y. Effect of plasma compression of plasma sheet stability [J]. *Geophys. Res. Lett.*, 1999, **26**(17):2705-2708

[101] Zhu P, Bhattacharjee A, Ma Z W. Hall magnetohydrodynamic ballooning instability in the magnetotail [J]. *Phys. Plasmas*, 2003, **10**(1):249-258

[102] Wong H V, Horton W, Van Dam J W, Crabtree C. Low frequency stability of geotail plasma [J]. *Phys. Plasmas.*, 2001, **8**(5):2415-2424

[103] Crabtree C, Horton W, Wong H V, Van Dam J W. Bounce-averaged stability of compressional modes in Geotail flux tubes [J]. *J. Geophys. Res.*, 2003, **108**(A2):1084, doi: 10.1029/2002JA009555

[104] Hurricane O A, Fong B H, Cowley S C, Coroniti F V, Kennel C F, Pellat R. Substorm detonation [J]. *J. Geophys. Res.*, 1999, **104**(A5):10 221-10 231

[105] Pritchett P L, Coroniti F V. Drift ballooning mode in a kinetic model of the near-Earth plasma sheet [J]. *J. Geophys. Res.*, 1999, **104**(A6):12 289-12 299

[106] Zhu P, Raeder J, Germaschewski K, Hegna C. Initiation of ballooning instability in the near-Earth plasma sheet prior to the 23 March 2007 THEMIS substorm expansion onset [J]. *Ann. Geophys.*, 2009, **27**(3):1129-1138

[107] Raeder J, Zhu P, Ge Y, Siscoe G. OpenGGCM simulation of a substorm: Axial tail instability and ballooning mode preceding substorm onset [J]. *J. Geophys. Res.*, 2011, **115**(A0): A00116, doi:10.1029/2010JA015876

[108] Leboeuf J N, Tajima T, Kennel C F, Dawson J M. Global simulations of the three-dimensional magnetosphere [J]. *Geophys. Res. Lett.*, 1981, **8**(3):257-260

[109] Brecht S H, Lyon J G, Fedder J A, Hain K. A simulation study of east-west IMF effects on the magnetosphere [J]. *Geophys. Res. Lett.*, 1981, **8**(4):397-400

[110] Wu C-C, Walker R J, Dawson J M. A three-dimensional MHD model of the Earth's magnetosphere [J]. *Geophys. Res. Lett.*, 1981, **8**(5):523-526

[111] Lyon J G, Fedder J A, Mobarry C M. The Lyon-Fedder-Mobarry (LFM) global MHD magnetospheric simulation code [J]. *J. Atmos. Solar Terr. Phys.*, 2004, **66**(15-16): 1333-1350

[112] Raeder J. Global MHD simulations of the dynamics of the magnetosphere: Weak and strong solar wind forcing [R]//Kan J R, Craven J D, Akasofu S-I ed. Substorms 2: Proceedings of the Second International Conference on Substorms, Fairbanks, Alaska, March 7–11, 1994. Fairbanks, Alaska; University of Alaska, Fairbanks. 1994. 561-568

[113] Raeder J, Larson D, Li W, Kepko E L, Fuller-Rowell T J. OpenGGCM simulations for the THEMIS mission [J]. *Space Sci. Rev.*, 2008, **141**(1-4):535-555

[114] Powell K G, Roe P L, Linde T J, Gombosi T I, De Zeeuw D L. A solution-adaptive upwind scheme for ideal magnetohydrodynamics [J]. *J. Comp. Phys.*, 1999, **154**(1):284-309

[115] Ogino T, Walker R J, Ashour-Abdalla M. A global magnetohydrodynamic simulation of the response of the magnetosphere to a northward turning of the interplanetary magnetic field [J]. *J. Geophys. Res.*, 1994, **99**(A6):11 027-11 042

[116] Palmroth M, Janhunen P, Pulkkinen T I, Peterson W K. Cusp and magnetopause locations in global MHD simulation [J]. *J. Geophys. Res.*, 2001, **106**(A12):29 435-29 450

[117] White W W, Schoendorf J A, Siebert K D, *et al.* MHD simulation of magnetospheric transport at the mesoscale [G]//Song P, Singer H J, Siscoe G L. Space

Weather, Geophysical Monograph Series Volume 125. Washington D C: America Geophys. Un. 2001. 229-240

[118] Winglee R M, Harnett E, Stickle A, Porter J. Multi-scale/multifluid simulations of flux ropes at the magnetopause within a global magnetospheric model [J]. *J. Geophys. Res.*, 2008, **113**(A2):A02209, doi 10.1029/2007ja012653

[119] Fedder J A, Slinker S P, Lyon J G, Elphinstone R D. Global numerical simulation of the growth phase and the expansion onset for a substorm observed by Viking [J]. *J. Geophys. Res.*, 1995, **100**(A10):19 083-19 093

[120] Wiltberger M, Pulkkinen T I, Lyon J G, Goodrich C C. MHD simulation of the magnetotail during the December 10, 1996, substorm [J]. *J. Geophys. Res.*, 2000, **105**(A12):27 649-27 663

[121] Raeder J, McPherron R L, Kokubun S, Lu G, Mukai T, Paterson W R, Sigwarth J B, Singer H J, Slavin J A. Global simulation of the Geospace Environment Modeling substorm challenge event [J]. *J. Geophys. Res.*, 2001, **106**(A1):381-395

[122] Siscoe G L, Kuznetsova M M, Raeder J. Search for an onset mechanism that operates for both CMEs and substorms [J]. *Ann. Geophys.*, 2009, **27**(8):3141-3146

[123] Hu B, Toffoletto F R, Wolf R A, Sazykin S, Raeder J, Larson D, Vapirev A. One-way coupled OpenGGCM/RCM simulation of the March 23, 2007 substorm event [J]. *J. Geophys. Res.*, 2010, **115**(A12), A12205, doi:10.1029/2010JA015360

[124] Ridley A J, Gombosi T I, Sokolov I V, Toth G, Welling D T. Numerical considerations in simulating the global magnetosphere [J]. *Ann. Geophys.*, 2010, **28**(8):1589-1614

[125] Toffoletto F, Lyon J, Sazykin S, Spiro R, Wolf D. RCM meets LFM: Initial results of one-way coupling [J]. *J. Atmos. Solar Terr. Phys.*, 2004, **66**(15-16):1361-1370

[126] Keller K A, Fok M C, Narock A, Hesse M, Rastaetter L, Kuznetsova M M, Gombosi T I, DeZeeuw D L. Effect of multiple substorms on the buildup of the ring current [J]. *J. Geophys. Res.*, 2005, **110**(A8):A08202, doi:10.1029/2004JA010747

[127] DeZeeuw D L, Sazykin S, Wolf R A, Gombosi T I, Ridley A J, Toth G. Coupling of a global MHD code and an inner magnetosphere model: Initial results [J]. *J. Geophys. Res.*, 2004, **109**(A12):A12219, doi:10.1029/2003JA010366

[128] Zhang J, Liemohn M W, DeZeeuw D L, Borovsky J E, Ridley A J, Toth G, Sazykin S, Thomsen M F, Kozyra J U, Gombosi T I, Wolf R A. Understanding storm-time ring current development through data-model comparisons of a moderate storm [J]. *J. Geophys. Res.*, 2007, **112**(A4):A04208, doi:10.1029/2006JA011846